UNITED STATES DEPARTMENT OF THE INTERIOR
GEOLOGICAL SURVEY

HYDROCARBON PROSPECTS FOR THE NAVARIN AND THE ALEUTIAN BASIN PROVINCES

by

M.S. Marlow and A.K. Cooper

Open-File Report 79-1667

This report is preliminary and has not been edited or reviewed for conformity with Geological Survey standards and nomenclature.

Menlo Park, California
October 1979

TABLE OF CONTENTS

SUMMARY

Recent seismic-reflection surveys reveal a frontier province of exceptional size--the Navarin basin province--beneath the northwestern Bering Sea shelf. Structural contours drawn on acoustic basement define three basins within the province; the basins contain strata 10 to 15 km thick and underlie more than 45,000 km^2 (11 million acres) of the Bering Sea shelf.

Tertiary mudstone dredged from the continental slope averages more than 0.25 percent organic carbon, and Cretaceous mudstone along the continental slope in Pribilof Canyon contains as much as 1 percent organic carbon. However, these beds may not be correlative with the lower basin sequences in the Navarin province because the stratigraphically lower beds wedge out against the flanks of the basin.

Eocene to Pliocene diatomaceous mudstones exposed on the continental slope have porosities ranging from 14 to 68 percent (average, 48 percent). Neogene reservoir beds may be present in the adjacent Navarin province because sedimentation has matched subsidence, which averaged 100 to 200 $m/10^6$ yr during Cenozoic time. Also, during Neogene time the Navarin basins were fed by major Alaskan and Siberian rivers, e.g., the Yukon, Kuskokwim, and Anardy rivers.

Large anticlinal structures in the northern half of the province that may have diapiric cores, structures associated with growth faults along the flanks of the basins' strata draped over basement blocks, and stratigraphic pinch outs and discordances in the basin fill, are all possible traps for hydrocarbons. Further exploration, including the drilling of stratigraphic test wells is needed to define this frontier province.

The Aleutian Basin is one of the three deepwater (more than 3,000m) sedimentary basins that lie north of the Aleutian Ridge. Several geologic and geophysical observations made by investigators working in the Aleutian Basin (summarized by Cooper and others, 1978), when considered collectively, suggest that the basin is a promising area for hydrocarbon exploration. Observations relevant to the existence of hydrocarbon accumulations include the following: 1) the basin contains a thick section of mostly Cenozoic sedimentary deposits (2 to 9 km thick) overlying an igneous oceanic crustal section; 2) potentially high thermal gradients exist in the sedimentary section; 3) structural features (diapirs, faults, basement ridges) are present throughout the basin; 4) the sedimentary section contains potential source and reservoir beds; and 5) within the central part of the basin are abundant VAMP's (velocity amplitude features), which may be caused by trapped gases within the sedimentary section.

INTRODUCTION

Since 1976 we have conducted two geological-geophysical expeditions along the Bering Sea continental margin and shelf in the vicinity of the U.S.-Russia Convention Line of 1867. In 1976 and 1977 we collected approximately 3600 km of 24 channel and single channel seismic-reflection data as well as lesser amounts of gravity, magnetic, bathymetric, and high-resolution seismic-reflection (1.0 kHz and 3.5 kHz) data (Fig. 1). In 1978, we collected single-channel sparker (160 kJ) seismic-reflection data along the margin and successfully occupied 20 dredge stations along the continental slope from west of the Pribilof Islands to the northwest towards Siberia. Publicly available data are shown by the track lines in Figure 2. A summary description of the dredge samples has been published by Marlow and others, 1979a.

The following sections are divided into three parts - the first section describes the geophysical exploration of Navarin basin, the results of dredging along the adjacent margin, and updates the petroleum geology of the area. The second part discusses the results of surveying in the deepwater areas of the Bering Sea basin. The final section gives recommendations for treaty negotiations concerned with the northern Bering Sea shelf and Aleutian basin.

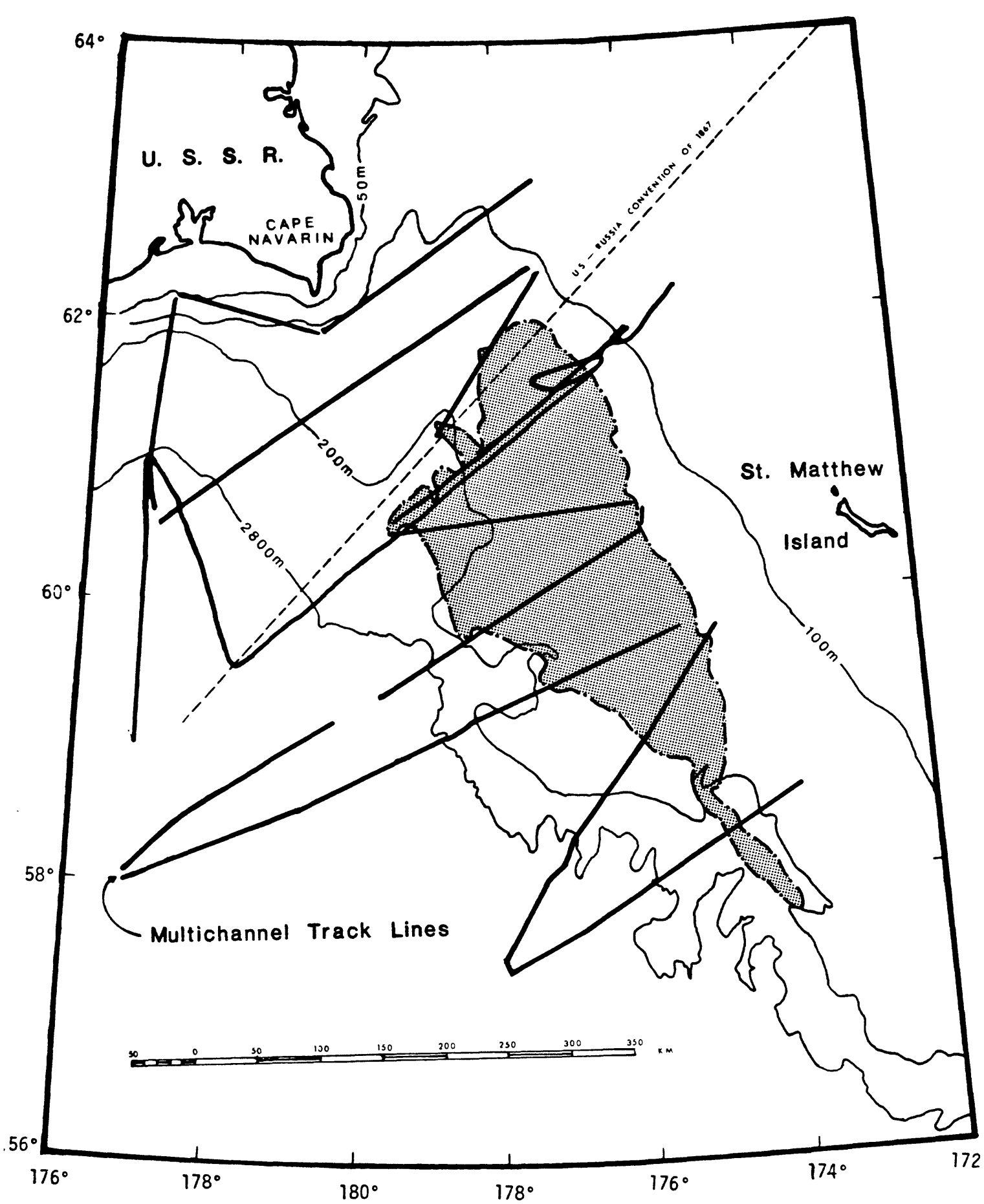

Figure 1. Tracklines of geophysical cruises conducted in 1976 and 1977. Heavy lines indicate coverage of 24 channel seismic-reflection data. Dashed and dotted line defines the Navarin basin province. Albers equal area projection.

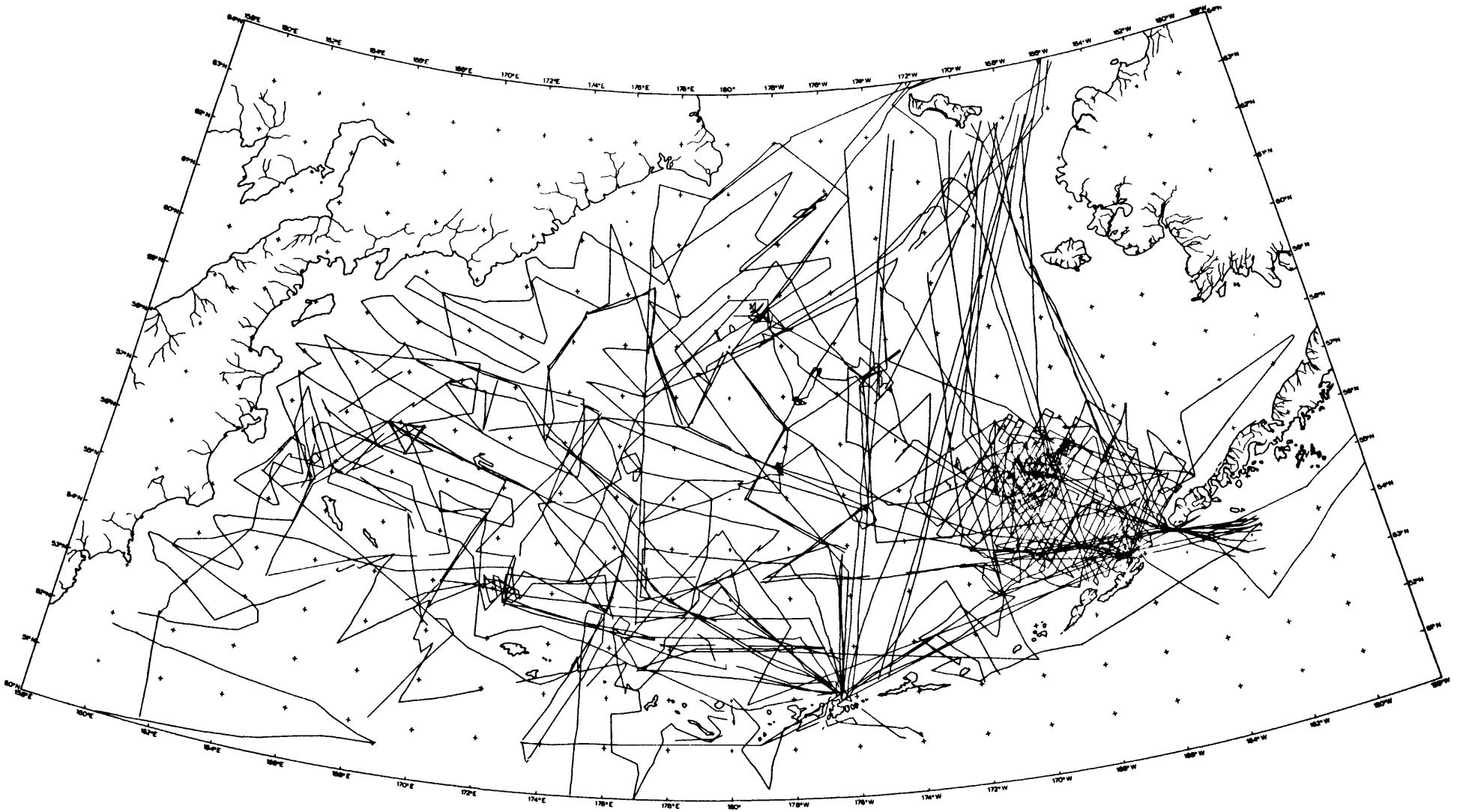

Figure 2. Tracklines of publicly available geophysical data for the entire Bering Sea region. Albers equal area projection.

NAVARIN BASIN PROVINCE AND BERING SEA MARGIN

Geophysical Exploration

In 1970 approximately 1000 km of single channel seismic-reflection records, using a 160-kJ sparker sound source, were collected in the Navarin province (Scholl and others, 1970). The reconnaissance records indicated that a thick stratified section underlies the northwestern Bering Sea shelf. Therefore, in their report based on these data, Marlow and others (1976) could only give a rough outline of the basin province. A more detailed outline of the basins, based on proprietary data, was included in our 1977 report.

During 1976 and 1977 surveys, 800 km of 24-channel seismic-reflection data were collected over the basin province proper using a sound source of five air guns totaling 1326 in^3. The multichannel data revealed that the Navarin basin province comprises a series of northwest-trending basins and ridges (Figs. 3,4) and that the stratified sequence in the basins is 10 to 15 km thick. To convert two-way traveltime on the seismic-reflection records to depths in meters of kilometers, we used a generalized velocity function.

$$D = 1.266t + 1.033t^2 - 0.117t^3$$

where

D = Depth or thickness in km

t = One-way traveltime

This function was derived by fitting a polynomial curve to velocity data from 150 sonobuoy stations in the Bering Sea. The velocity function used here supersedes the curve published by Marlow and others (1976).

Although Mesozoic beds may form part of the basin fill, the greater part

of the sequence is probably of Cenozoic age. The sedimentary beds in the southern two basins are undeformed except along the flanks of the basin, where reflectors are cut by normal faults. The sedimentary section in the northern basin is folded into large anticlines 10 to 15 km wide that may have diapiric cores (profile C-D, beneath the late Miocene-Pliocene unconformity, Fig. 5). Geophysical coverage of the Navarin province northwest of the 1867 U.S.-Russia Convention Line is limited to a few lines taken by the U.S. Geological Survey (no proprietary data exists for the Soviet side of the line), and hence, the size and extent of the folded beds are unknown.

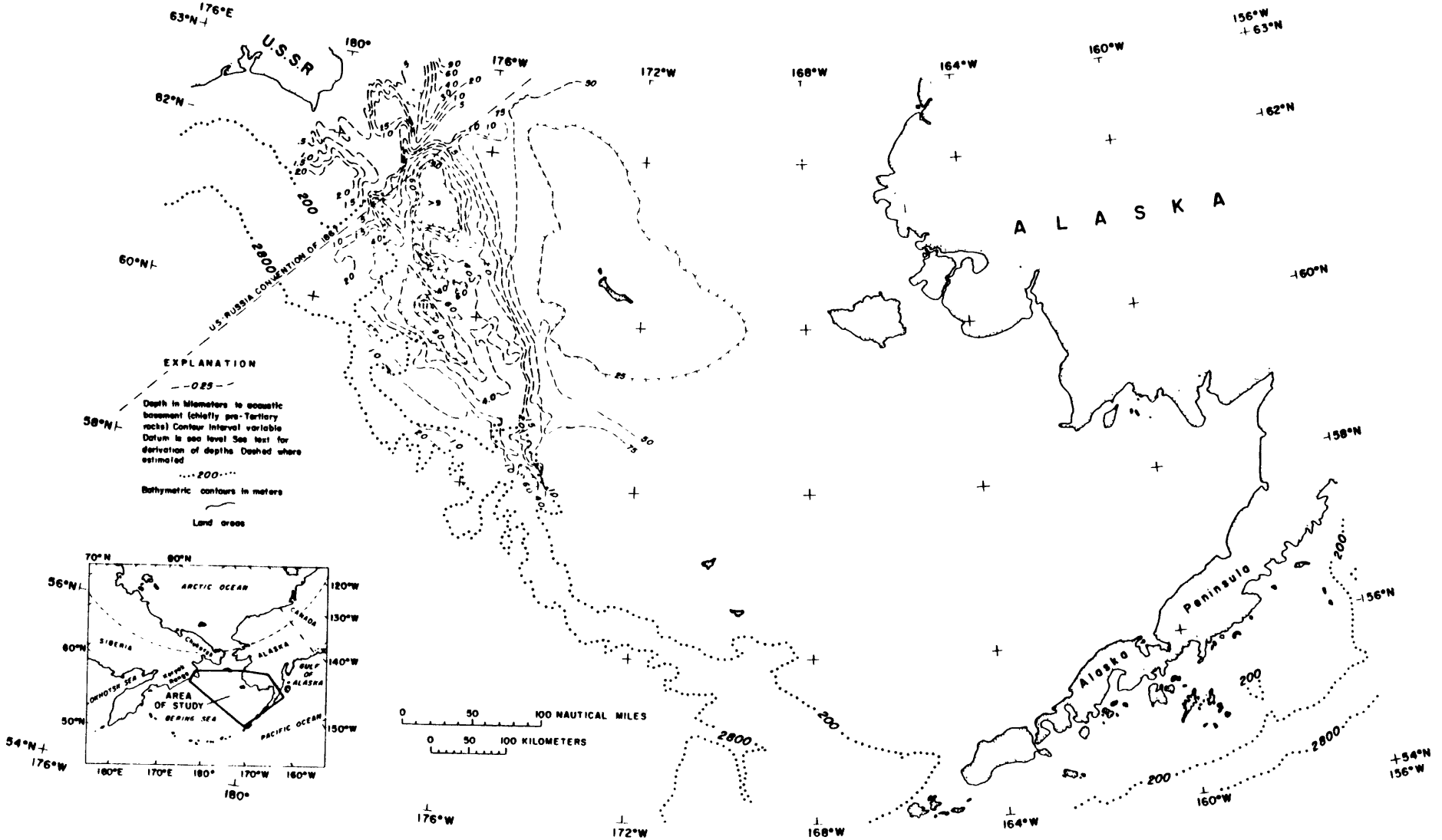

Figure 3. Structural contours of acoustic basement. Derived in part from Marlow and others (1976, 1977). See text for explanation.

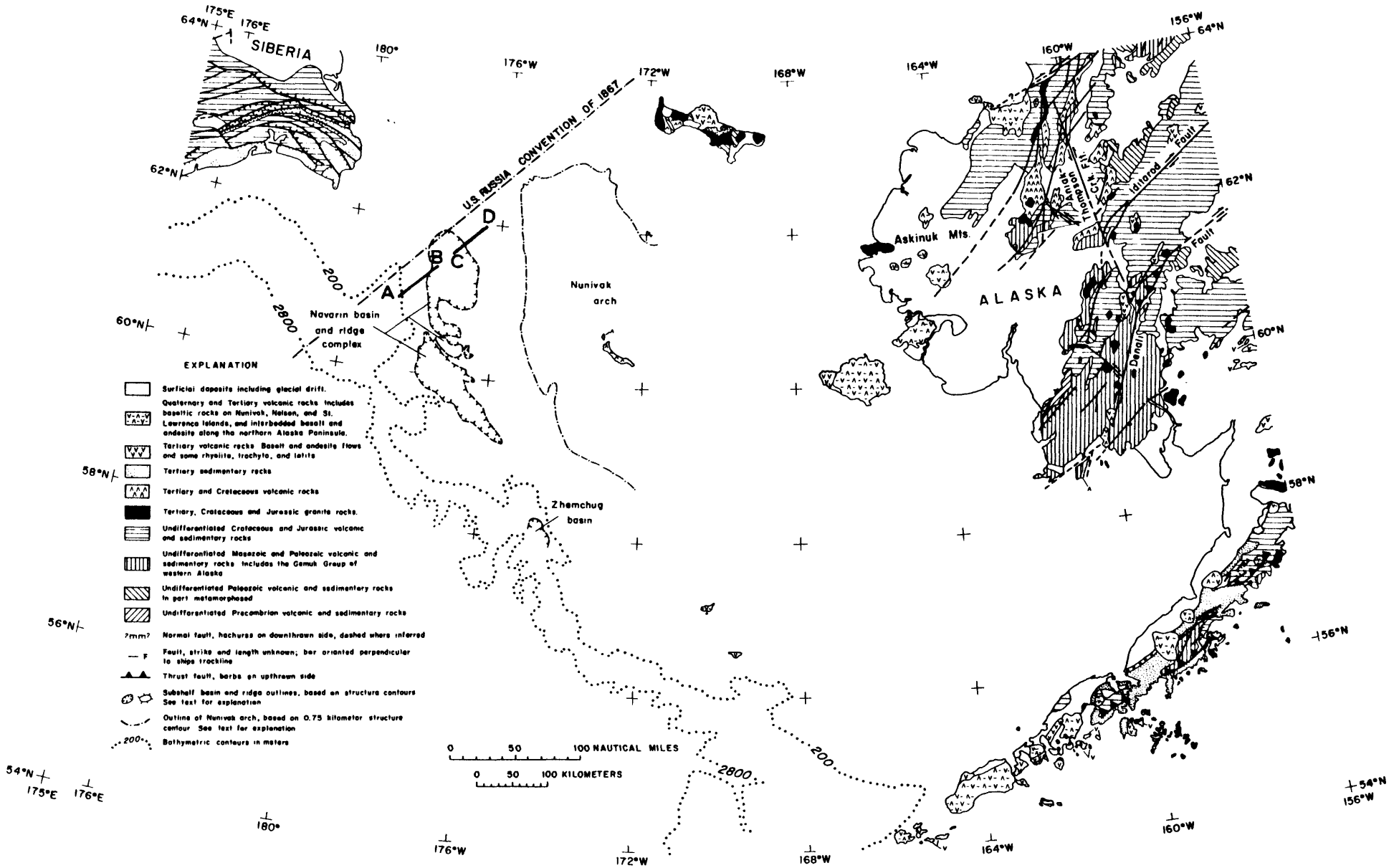

Figure 4. Outline of the Navarin basin province and Nunivak arch (a basement high) based on the structural contours on acoustic basement shown in Figure 3. Generalized geology of western Alaska, the Alaska Peninsula, and eastern Siberia is from Burk (1965), Yanshin (1966), and Beikman (1974, 1978). Note location of seismic-reflection profiles A-B and C-D shown in Figure 5.

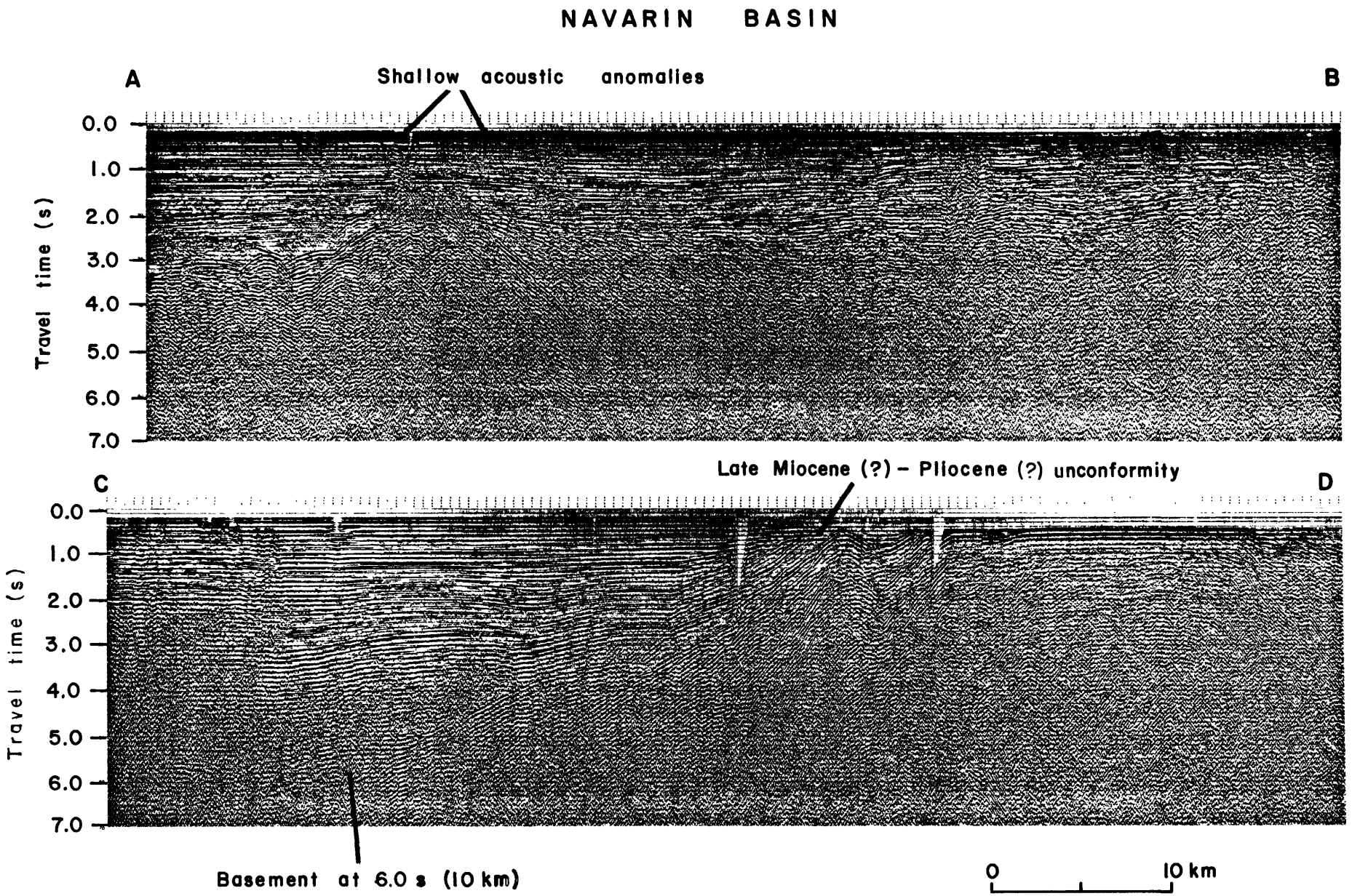

Figure 5. 24 Channel seismic-reflection profiles A-B and C-D. Travel time is two-way and profile locations are shown in Figure 4.

Geological Exploration

During 1978 twenty dredge sites were occupied and successfully dredged from the R/V S.P. LEE along the eastern Bering Sea continental margin (Fig. 6). A total of several tons of rock were collected using a chain-bag dredge. Samples were recovered in water depths ranging from 750 to 2,750 meters from exposures along the continental slope bordering the large Bering Sea shelf. A preliminary petrographic description of the major lithologies recovered at each station is given in Table 1. At one locality, station L5-78-BS-5, rocks probably recovered from acoustic basement contain the megafossil, Buchia rugosa, of Kimmeridigian or Late Jurassic age. Similar lithic volcanic sandstones were recovered at eight other sites, L5-78-BS-2, -4, -6, -8, -13, -21, -22, and -27. These samples are also thought to be from the basement complex beneath the margin, but, unfortunately, these rocks did not yield diagnostic fossils. The basement strata are overlain unconformably by diatomaceous mudstone or sandstone as old as Late Eocene or early Oligocene.

Seismic-reflection and gravity data indicate that the basement rocks beneath the margin are part of a belt of interconnected ridges that extend from the western tip of the Alaska Peninsula northwest to Siberia, a distance of nearly 1,250 km (Marlow and others, 1979c).

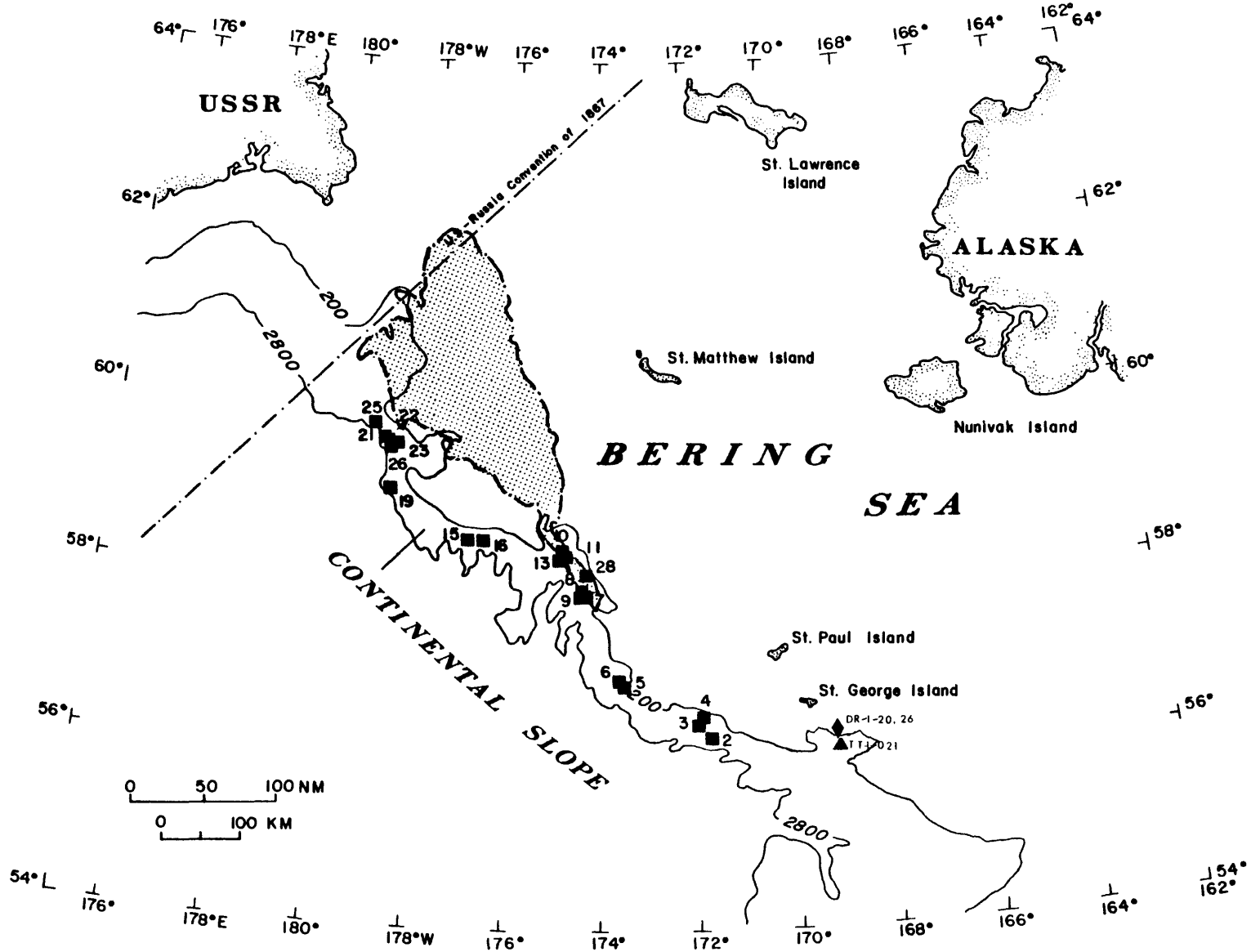

Figure 6. Location of dredge sites along the Bering Sea continental slope Site TT-1-021 is from Hopkins and others (1969) and sites DR-1-20 and DR-1-26 (Upper Jurassic sandstone) are from T. Vallier (personal comm., 1979).

Table 1. Preliminary petrographic description of dredge samples from the Bering Sea continental margin

Dredge	Station	Latitude	Longitude	Depth (meters)	Lithology	Age
L5-78-BS	2-2	56°12.3'N	171°42.2'W	2500-2700	Volcanic sandstone	
	2-4	"	"	"	Diatomaceous mudstone	Late Oliogocene
	2-5	"	"	"	Diatomaceous sandy mudstone	Early Miocene
	3-1	56°22.0'N	171°53.4'W	2000-2200	Volcanic sandstone	
	4-1	56°25.6'N	171°53.5'W	1550-1700	Diatomaceous mudstone	Early Oligocene (?)
	4-2	"	"	"	Volcanic sandstone	
	5-1	56°51.1'N	173°32.7'W	1500-1700	Diatomaceous mudstone	Late Oligocene
	5-5	"	"	"	Volcanic sandstone	Late Jurassic
	5-7	"	"	"	Micritic limestone	Late Middle Miocene
	6-7	56°50.5'N	173°31.4'W	1600-1850	Diatomaceous mudstone	Late Oligocene to Early Miocene
	6-9	"	"	"	Volcanic sandstone	
	6-16	"	"	"	Graywacke	Pleistocene
	7-3	57°53.0'N	171°22.3'W	1600-1900	Diatomaceous mudstone	Early Middle Miocene
	8-1	57°53.1'N	174°22.6'W	1250-1500	Diatomaceous mudstone	Late Miocene
	8-6	"	"	"	Diatomaceous mudstone	Middle-Middle Miocene
	9-2	57°52.0'N	174°25'W	1200-1250	Glauconitic mudstone	Late Middle Miocene
	9-3	"	"	"	Micritic limestone	Early Pliocene
	11-1	58°20.1'N	174°51.6'W	1400-1550	Micritic diatomaceous mudstone	Middle-Middle Miocene
	13-2	58°19.73'N	"	750-1100	Micritic limestone	Late Pliocene
	13-3	"	"	"	Volcanic sandstone	
	15-2	58°27.5'N	176°51.9'W	950-1100	Micritic limestone	
	15-3	"	"	"	Tholeiitic basalt	Minimum age = 54.7± 1.08 m.y.*
	16-2	58°28.6'N	176°36.5'W	1800-2050	Basaltic tuff	
	16-6	"	"	"	Muddy limestone	Eocene
	16-9	"	"	"	Mudstone	Late Early to Early Middle Eocene
	19-2	59°03.3'N	178°43.1'W	1500-2500	Mudstone	Late Quaternary
	21-1	59°38.5'N	178°52.2'W	1800-2600	Volcanic siltstone	Tertiary to Recent
	21-2	"	"	"	Volcanic sandstone	

21-3	"	"	"	Metagabbro	
21-5	"	"	"	Andesite tuff	
22-2	59°36.9'N	178°49.2'W	1500-2200	Glauconitic sandstone with andesite clast	
22-4	"	"	"	Micritic limestone	Late Miocene to Quaternary
22-13	59°36.9'N	178°49.2'W	1500-2200	Latite or Dacite	
22-17	"	"	"		
25-2	59°47.2'N	179°08.3'W	2000-2800	Tuff	Quaternary
26-1	59°33.8'N	178°47.4'W	1800-2500	Volcanic sandstone	Early Pliocene
26-2	"	"	"	Mudstone	
26-4	"	"	"	Tuff (replaced by calcite)	
26-6	"	"	"		
27-1	59°36.2'N	178°38.8'W	1750-1800	Sandy siltstone interbedded with volcanic sandstone	Possibly Eocene
27-2	"	"	"	Volcanic sandstone	
28-1	58°66.1'N	174°18.3'W	800-1650	Sandy mudstone	Late Miocene
28-3	"	"	"	Sandy limestone	Late Miocene to Early Pliocene
28-E3	"	"	"	Volcanic sandstone	

* $K_2O = 2.189, 1.191\%$

$^{40}Ar_{rad}/gm = 1.752 \times 10^{-10}$ moles/gm

$$\frac{^{40}Ar_{rad}}{^{40}Ar_{total}} = 0.8453$$

Apparent minimum (sample altered) age using K^{40} decay constants of: $= 4.962 \times 10^{-10}$/yr; $= 8.78 \times 10^{-13}$/yr; abundance ratio: $^{40}K/K = 1.1676 \times 10^{-4}$ atom percent

Source Beds

The Navarin basin province has not yet been drilled or sampled; thus little is known about possible source beds in the province's sedimentary section. Rocks dredged from the Beringian continental slope west and southeast of the Navarin province include lithified volcanic sandstone at Late Jurassic age, mudstone of Late Cretaceous age, and less consolidated deposits of early Tertiary age (Fig. 6). Geochemical analyses and the physical properties of some of these rocks are listed below:

Table 2. Geochemical analyses and physical properties of rocks dredged from the Bering Sea continental margin. See Figure 6 for locations.

Sample number	Lithology	Age	Organic carbon (Wt.%)	Pyrolytic hydro carbon (Wt%)	Vitrinite reflectance (Avg. %)	Porosity (%) perm. (md)
S6-77-BS						----/----
DR1-20	Volcanic sandstone	Late Jurassic	0.79	0.24	.38	
DR1-26	Volcanic sandstone	Late Jurassic	0.26	0.01	1.14	----/----
TT-1-021						
001	Mudstone	Late Cretaceous	0.62	0.11	.40	----/----
L5-78-BS						
5-5	Sandstone	L.Jurassic	.27	.02	.63	----/----
2-3	Mudstone	Paleogene	.33	.02	.41	----/----
16-9	Mudstone	M. Eocene	.83	.04	.31	----/----
2-4	Mudstone	L.Oligocene	-	-	-	68.3/5.46
2-11	Siltstone	L.Oligocene	-	-	-	45.1/1.25
5-10	Tuff	L.Oligocene	-	-	-	50.7/19.0
7-3	Mudstone	M.Miocene	-	-		57.4/1.67

Pyrolytic analyses of these rocks indicates that none are good source beds for petroleum, with the possible exception of the Cretaceous mudstone (Sample # TT-1-021-001) and one Upper Jurassic sandstone (Sample #S6-77-BS-DR-

1-20). However, the mudstone was dredged from the continental slope in Pribilof Canyon, 500 km southeast of the Navarin province. The outcrops sampled by rock dredging are generally sandy units that may not be representative of finer-grained possible source beds that are exposed either along the margin or lie within the sub-shelf basins. Also, many of these dredge samples are from exposures that crop out too far down on the continental slope to be representative of the lower sediment sections in the basins of the Navarin province.

Reservoir Beds

The porosities of Oligocene to Pliocene rocks dredged from eight sites along the Bering Sea continental margin range from 14 to 68 percent (avg. 48 percent). These Tertiary samples are generally very porous - probably because of abundant diatom frustules. The permeability of the four samples tested is variable, no doubt due to submarine weathering and cementation. Tertiary outcrops can be traced as seismic reflectors to the subshelf basins, where, if the beds remain diatomaceous, good potential reservoir beds may occur.

Neogene reservoir rock beds of shallow-water origin are likely to be present in the Navarin basins because sedimentation has matched subsidence, which averaged 100 to 200 $m/10^6$ yr during Cenozoic time. The thick sections of these basins beneath the Bering Sea shelf accumulated near the mouths of major Alaskan and Siberian rivers, including the Yukon, Kuskokwim, and Anadyr. During Neogene time, the shelf was swept by numerous marine transgressions and regressions (Hopkins, 1967; Hopkins and Scholl, 1970). All these factors suggest the likely deposition of neritic and deltaic strata.

The stratigraphically lower sections of the basins are presumed to include upper Mesozoic and lower Tertiary beds. The geologic evolution of the Bering Sea shelf and margins suggests that in late Mesozoic and early Tertiary time, the then-forming shelf basins were flanked by coastal mountains, peninsulas, and islands. These subsiding, yet relatively high, land masses of Mesozoic rock probably shed coarse clastic debris to the adjacent basins during early Tertiary time.

Traps

Strata in the northern basin of the Navarin province are folded into anticlinal structures 10-15 km across (Fig. 5); this folding may have been caused either by diapirism or by lateral compression. Only three survey lines cross the folds here, and the size and extent of the folds are unknown. The anticlines are cut or folded by an unconformity that is overlain by a few tens of meters of flat-lying strata. High-amplitude reflection events are observed within the strata above the balded folds. Beds in the southern two basins are cut by normal faults along the flanks of the basins. Increase in the offset across these faults with depth indicates that the faults are growth structures that formed contemporaneously with basin filling.

Potential stratigraphic traps also exist within the Navarin basins. For example, beds in the lower basin fill thin toward the basement flanks of the basin and generally dip toward the basin axis, so that fluids migrating updip could be trapped against denser, less permeable rocks of the Mesozoic basement. In addition, the lower stratigraphic sequence in the basin is often overlapped discordantly by the younger overlying beds. Thus hydrocarbons moving updip along the lower beds could be contained by impermeable layers in the upper flat-lying strata.

Other potential traps for hydrocarbons in the Navarin province include drape structures, i.e. strata in the bottom of the three basins often are draped over blocks in the basement and this closure could form potential traps for migrating fluids from the basement complex. Some of these features are quite large - offset on the basement blocks often is several thousand meters and the blocks extend laterally more than 5-10 km.

Summary

The Navarin basin province is a recently discovered frontier shelf area of significant hydrocarbon potential. Though relatively unexplored and unknown, the province underlies at least 45,000 km^2 (11 million acres) of the shelf and comprises three large basins. The sedimentary sequences filling the basins are 10 to 15 km thick. Although Cretaceous units may form part of the stratified sequences, most of the section is probably of Cenozoic age.

Reconnaissance geophysical data reveal anticlinal or diapiric(?) structures, stratigraphic pinchouts, and growth faults within the basins. Discoveries of oil and gas in Tertiary beds in nearby Siberia encourage speculations that hydrocarbon deposits occur in the Navarin basins. The vast size of these basins statistically argues for the presence of oil and gas beneath the northwestern Bering Sea shelf.

Further exploration of the Navarin basins and the adjacent continental slope is needed. Seismic-reflection, and seismic-refraction surveys, as well as gravity and magnetic data are especially needed to understand the geologic history of these large structures. Samples obtained by dredging on the continental slope and by direct drilling in the basins may confirm the existence of suitable source and reservoir beds within the Navarin province.

ALEUTIAN BASIN PROVINCE

Introduction

The Bering Sea continental margin extends 1300 km northwest from the Aleutian Ridge to Cape Navarin, Siberia. The outer margin which, includes the outer continental shelf, the continental slope, Umnak Plateau and the continental rise, is cut by several immense submarine canyons. Thick accumulations of Cenozoic strata are found along the sediment-draped parts of the continental slope as well as beneath the abyssal Aleutian Basin. The transition from continental crust, which is incised by deep shelf basins, to oceanic crust, which is covered by thick sediment, occurs beneath the continental slope.

The Aleutian Basin is the deep water (greater than 3,000 m) basin that lies north of the Aleutian Islands adjacent to the Bering Sea continental shelf. The basin, about the size of Texas, is underlain by a 2-9 km-thick flat-lying sequence of mostly Cenozoic sediment that rests on an igneous oceanic crustal section. Prior to 1974, marine investigations in the Aleutian Basin were directed at understanding the basin's regional geologic and geophysical framework; more recent investigations by the U.S. Geological Survey have been aimed at assessing the basin's hydrocarbon potential. Preliminary results suggest that the four major requirements for hydrocarbon accumulations may be present, namely structural and stratigraphic traps, source rocks, reservoir beds, and an adequate thermal and sedimentation history.

The recent energy resource studies indicate that: 1. numerous structural features (gentle folds, diapirs, basement ridges) are present in the central

and eastern parts of the basin; 2. acoustic features called VAMP's (Velocity Amplitude features) are common (over 350 identified) in the central basin; these features may be caused by pockets of gases and possibly other hydrocarbons that have been trapped in the sedimentary section; 3. the sedimentary section consists of diatomaceous sediment overlying indurated mudstones; high porosities (58%-85%) and good permeabilities (10-35 millidarcy) in the diatomaceous sediment suggest it is a potential reservoir unit while the thick section of underlying mudstone may contain source beds; 4. concentrations of organic gases, primarily methane, in the upper 1-3 meters beneath the seafloor are very small, they increase with depth, and they are highest in areas near VAMP's, and; 5. the thermal gradient and the sediment thickness are sufficiently large to allow hydrocarbon maturation at depth, if suitable organic material is present.

Our initial results suggest that the Aleutian Basin deserves further exploration as a site for possible hydrocarbon accumulations.

Overview

Excellent syntheses of the Bering Sea Basin and surrounding areas have been given by Ewing and others (1965), Stone (1968), Gnibidenko (1973), Scholl and Creager (1973), Ludwig (1974), Scholl and others (1975), and Cooper and others (1977c); a brief summary of the ideas presented in these papers is given here.

The Bering Sea Basin, typical of many other marginal basins surrounding the Pacific Ocean, contains a thick (2-9 km) section of mostly Cenozoic sediment impounded behind an outer island arc, the Aleutian Ridge (Fig. 7). Except for the great thickness of the overlying sedimentary section, the crustal structure of the basin is geophysically similar to an oceanic rather than a continental area. This similarity along with other geologic and geophysical data from both the basin and from surrounding areas, suggests that the area may have been part of the North Pacific Ocean before Late Mesozoic (60-70 m.y.) time. At the end of the Mesozoic Era, the initial development of the Aleutian Ridge fractured the oceanic plate (Kula plate) and isolated a segment of oceanic crust on the north side of the newly formed ridge. The growth of the two interior submarine ridges, Bowers and Shirshov Ridge (Fig. 7), may also have started at this time. Since Late Mesozoic time, terrigenous and pelagic sediment have continued to drape the continental slopes and fill the Aleutian and Bowers basins with a nearly flat-lying section of sedimentary rock.

Geologic Data

Geologic sampling of surface sediment in the Aleutian Basin (Hanna, 1929; Lisitsyn, 1966; Gershanovich, 1968; Frazer and others, 1972; Anonymous, 1977) indicates that the primary constituent is siliceous mud, with varying amounts of interbedded terrigeneous material depending on the proximity of the

sampling site to shallow regions. The upper 627 meters of the basin's sedimentary fill was drilled at DSDP site 190 (Fig. 7) and has been described by Creager, Scholl and others (1973) and Scholl and Cooper (1978). Three sedimentary units were penetrated - an upper 375-meter-thick unit of diatomaceous silty clay with interbedded turbidites (Holocene through Late Pliocene), a middle 240-meter-thick unit of semi-indurated diatomaceous silty clay (Late Pliocene through upper Miocene), and a lower unit of indurated mudstone of unknown thickness (upper middle Miocene).

Acoustic basement (basalt?) has not been reached at drilling sites within the thick sedimentary section of the Aleutian and Bowers Basins; consequently, the age and lithology of the greater part of the section (1-7 km) are unknown. Regional geologic considerations and rock samples collected along the continental slope (Scholl and other, 1966; Hopkins and others, 1969), led Scholl and others (1975) to suggest that the oldest sedimentary rocks overlying acoustic basement may be of late Mesozoic or early Tertiary age. However, the identification of Early Cretaceous seafloor spreading anomalies in the Aleutian Basin (Cooper and others, 1976a, b, c) supports the notion that the lower Cretaceous sedimentary units may lie at the base of the sedimentary section.

Geophysical Data

Single-channel seismic-reflection profiles recorded in the Bering Sea Basin (Ewing and others, 1965; Ludwig and others, 1971a; Creager, Scholl and others, 1973; Scholl and others, 1976; Rabinowitz and Cooper, 1977; Cooper, unpublished records) indicate an internally reflective and well-stratified layer overlying a deeper acoustically opaque unit. Seismic-refraction surveys

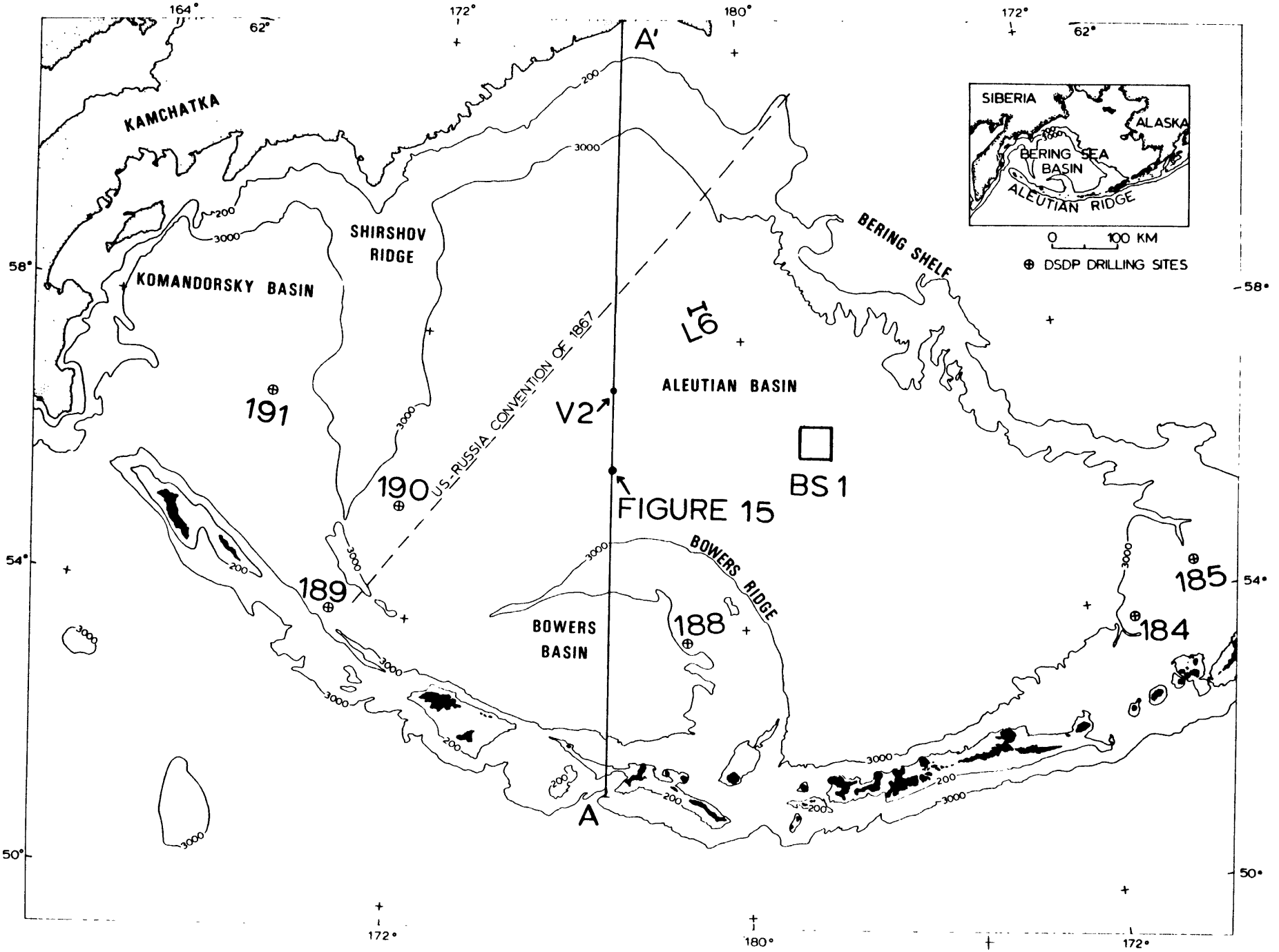

Figure 7. Index map of the Bering Sea Basin. Bathymetric contours in meters. Transverse mercator projection.

(Shor, 1964; Houtz and others, 1970; Ludwig and others, 1971b; Hamilton and others, 1974; Rabinowitz and Cooper, 1977; Childs and Cooper, 1979) confirm that the change in reflective units generally coincides with a well defined refraction horizon (2.7-2.9 km/sec) that separates overlying lower velocity units (1.5-2.0 km/sec) from underlying higher velocity (3.5-4.7 km/sec) layers. The refraction data also confirm that the basin's thick sedimentary sequence is underlain by oceanic crust. This crust consists of a 1-2 km-thick layer with a velocity of 5.0-6.0 km/sec (oceanic layer 2), a 2-6 km-thick layer with a velocity of 6.6-7.2 km/sec (oceanic layer 3) and a high-velocity layer of 7.5-8.2 km/sec (mantle). Figure 8 shows a refraction velocity structure section that extends across the Bering Sea Basin. Multichannel seismic-reflection data have also been recorded along part of the structure section (MCS Line 44, Cooper and others, 1977b); these and other unpublished multichannel data (authors' files) confirm the great thickness of sedimentary beds (2-9 km) that fill the basin. These data also reveal folded and faulted sections along the north side of Bowers Ridge and at the base of the continental slope in the eastern Aleutian Basin.

Magnetic surveys in the Bering Sea Basin (Vorobev, 1970; Kienle, 1971; Soloveva, 1968; Regan and others, 1975; Cooper and others, 1975; Cooper and others, 1976a, b; Cooper and others, 1977c) illustrate two distinct types of anomalies. The first type is a set of narrow 25-100 km-wide linear anomalies believed to have been formed by seafloor spreading (Cooper and others, 1976b). The second type is a long-wavelength negative anomaly centered over the Aleutian Basin (Regan and others, 1975; Cooper and others, 1977c), an anomaly thought to be related to deep-seated thermal activity beneath the basin (Cooper and others, 1977c).

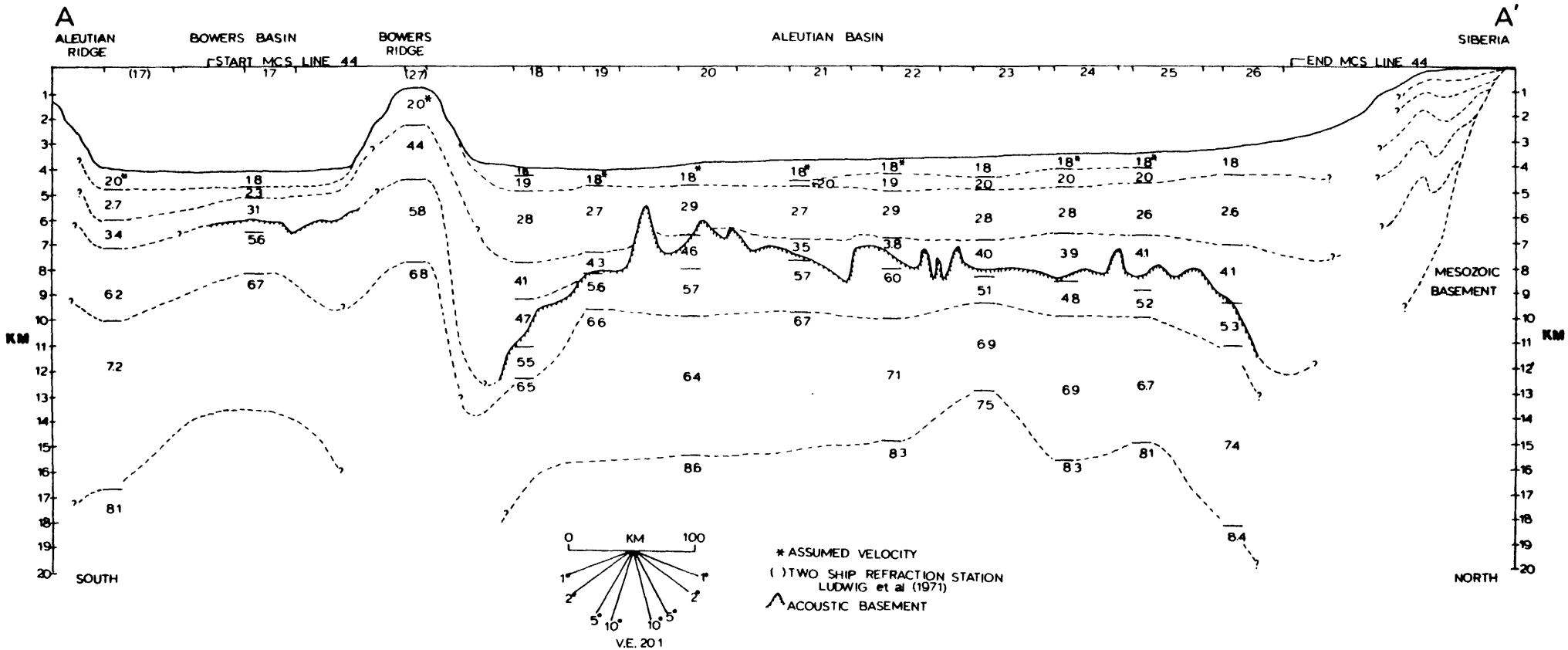

Figure 8. Crustal structure section (A-A') across the Bering Sea Basin; see Figure 7 for location. The abyssal basins have an oceanic crustal section consisting of layers of diatomaceous sediments (1.8-2.0 km/sec), indurated mudstones (2.6-2.9), other sedimentary units (3.5-4.7), acoustic basement (oceanic layer 2 basalt? 4.8-6.0), oceanic layer 3 (6.4-7.4), and mantle (7.5-8.6). Note the regional thinning of the sedimentary section toward the center of the Aleutian Basin. Acoustic basement depths are from U.S.G.S. Multichannel seismic (MCS) line 44 recorded in 1976. Unless otherwise indicated, all velocities (km/sec) are unreversed refraction velocities from sonobuoys recorded along MCS line 44.

Published gravity data (Kienle, 1971; Watts, 1975) reflect the presence of both the large submarine ridges (gravity highs) and the thicker sections of sedimentary beds that underlie the perimeter of the basin (gravity lows). Broad low-amplitude anomalies are in the center of the basins and are the result of regional variations in either the depth to igneous basement or in the thickness of the oceanic crust (Cooper and others, 1977c).

Several heat flow measurements have been made in the Bering Sea Basin (Foster, 1962; Erickson, 1973; Watanabe and others, 1977; Marshall and others, 1978). Watanabe and others (1977) report an average heat flow of 1.44 ± 0.22 $cal/cm^2/sec$ for the Aleutian Basin, a value that is compatible with the predicted heat flow for Mesozoic oceanic crust. A regional correlation of higher heat flow values with broad magnetic anomalies in the central and eastern Aleutian Basin is noted by Cooper and others (1977c) and is believed to result from higher subcrustal temperatures in these areas.

Hydrocarbon Exploration

Prior to 1974, the primary interest of investigators working in the Bering Sea Basin was to decipher the basin's regional geologic and tectonic history. More recent studies have been directed toward evaluating the hydrocarbon potential of the basin. The recent studies indicate that four of the important factors generally required for the accumulation of hydrocarbon deposits may be present: (1) adequate structural or stratigraphic traps, (2) an appropriate thermal and sedimentation history, (3) source rocks, and (4) reservoir beds. Several observations made since 1974 have contributed to this conclusion.

A. Recognition of marginal basins in general as potential hydrocarbon

accumulation areas (Schlanger and Combs, 1975);

B. Identification of acoustic features (VAMP's) within the sedimentary section which may be associated with low-velocity, gas-saturated sediment (Cooper, 1974; Scholl and Cooper, 1978);

C. Identification of a possible thermal anomaly beneath the central Aleutian Basin (Cooper and Scholl, 1974; Cooper and others, 1977c);

D. Identification of structural features, such as intrabasin faults, basement ridges, and diapirs, features that are often associated with VAMP's (Cooper, 1977; Cooper and others, 1977a; Cooper and others, 1979).

E. Recognition of suitable organic carbon content and organic gases in sedimentary deposits of the Bering Sea Basin (Gershanovich, 1968; Bode, 1973; Claypool and others, 1973; Marlow and others, 1976; Underwood and others, 1979).

Structural and Acoustic Features

The abundance of Velocity Amplitude features (VAMP's), the deep-water equivalent of seismic "bright spots" (Scholl and Cooper, 1978), throughout the Aleutian Basin is the strongest evidence that structural and stratigraphic traps may be present within the upper part of the sedimentary section. VAMP's appear on both the single-channel and multichallen seismic data (Fig.9) and are characterized by columns of concave-upward reflectors that often increase in amplitude with depth, high-amplitude reflections and phase reversals immediately above the columns, and structural upbowing of the beds and seafloor immediately above the feature. Scholl and Cooper (1978) interpret the VAMP's as resulting from a low-velocity zone of gas-charged deposits and possibly other hydrocarbon products within the upper part of the sedimentary

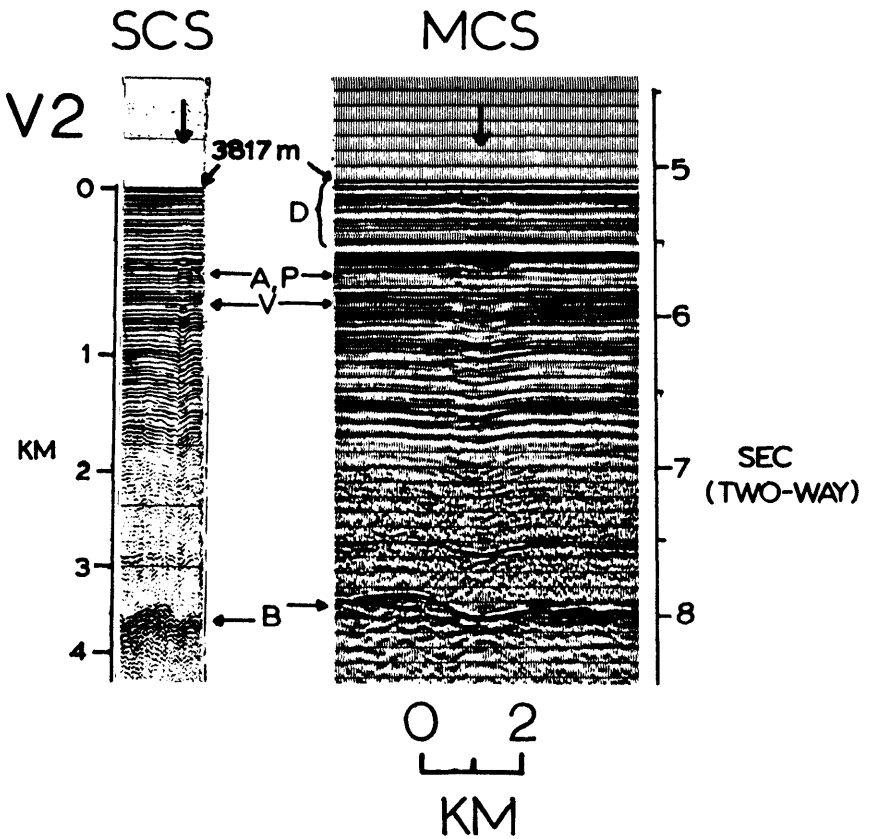

Figure 9. Example of a typical Velocity-AMPlitude feature (VAMP), V2, shown on both a single-channel seismic (SCS) and 24-fold multichannel seismic (MCS) record; see Figure 7 for location. Disturbed reflectors (D) lie above the top of the VAMP, which is marked by a phase inverted (P) increased amplitude (A) reflector. A velocity pulldown (V) appears beneath reflector "A, P" and increases in magnitude (time delay increases from 0.0 to 0.1 sec) downsection to and including the acoustic basement reflector (B). VAMP V2 has been cored at station 6 (Figure 13). Depth scale from Cooper and others (1977a).

section. Detailed surveys show that VAMP's often occur over the top of basement ridges (Fig. 10) but are not always related to basement topography (Fig. 9). Pseudostructural relief on the acoustic basement is observed in the time base reflection profiles across some VAMP's. The small depression (0.15 sec) in the basement reflector beneath VAMP V2 (Fig. 9) results mostly from the time delay caused by the low-velocity deposits near the top of the VAMP.

The isopach map of the sedimentary section above acoustic basement (Fig. 11) indicates that large local variations in sediment thickness exist beneath the central and eastern parts of the Aleutian Basin. Because the seafloor is the abyssal areas is nearly flat, these local variations reflect undulations in the acoustic basement surface. Folding and faulting of sedimentary horizons are commonly found over buried basement relief such as ridges, isolated knolls and domes, and fault-displaced basement rocks. A typical example of a large (3 km relief) buried basement feature, Sounder ridge, is located in the eastern Aleutian Basin. Profile L6 (Fig. 12) reveals that the sedimentary section above the ridge is folded, the seafloor is uplifted, and faulted reflectors occur at depth along the ridge flanks. Sounder ridge, as well as other ridges in the eastern Aleutian Basin, has a complex history of growth. The difference in acoustic character of the reflectors and the difference in the total sediment thickness on the northwest and southeast sides of the ridge imply that the ridge is an old feature (early Tertiary?) that has acted as a long-term sediment barrier; structural deformation of the shallow sediment and seafloor suggest a renewal of ridge growth in Late Cenozoic time.

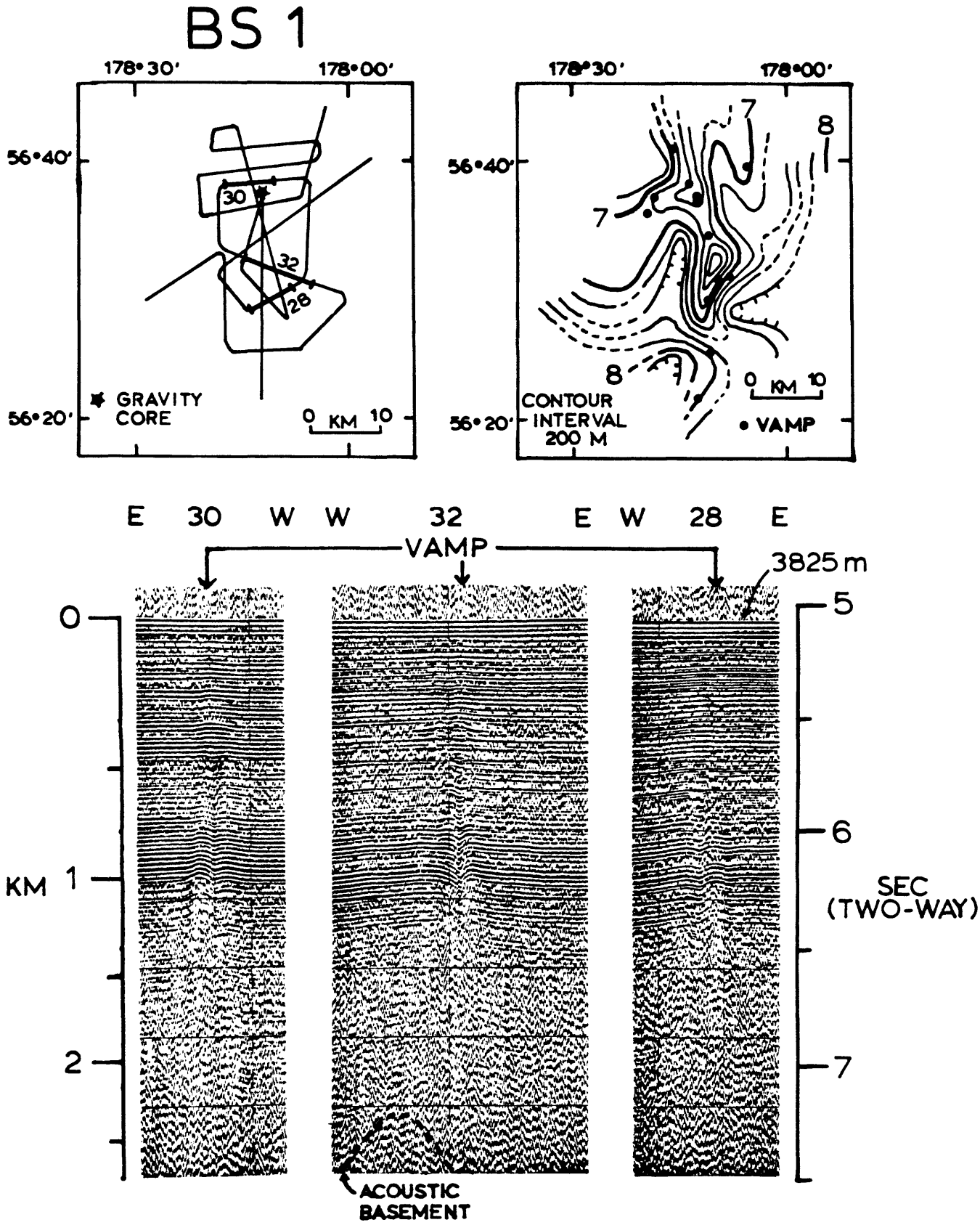

Figure 10. Box Survey (BS1) over an area of VAMP's; see Figure 7 for location. The contour map (upper right) gives the total depth (km) from sea level to acoustic basement. In the three traverses, the VAMP's occur over the top of a buried basement ridge that has a relief of nearly 1500 meters. The upbowing of reflectors directly above the VAMP along line 32 is also seen as a 2-meter upbowing of the sea-floor in high resolution bathymetric profiles (not shown). Here, the VAMP's appear to be related to basement relief, whereas in Figure 9, the VAMP is not. The VAMP along line 30 has been cored at Station 2 (see Figure 13). Depth scale from Cooper and others (1977a).

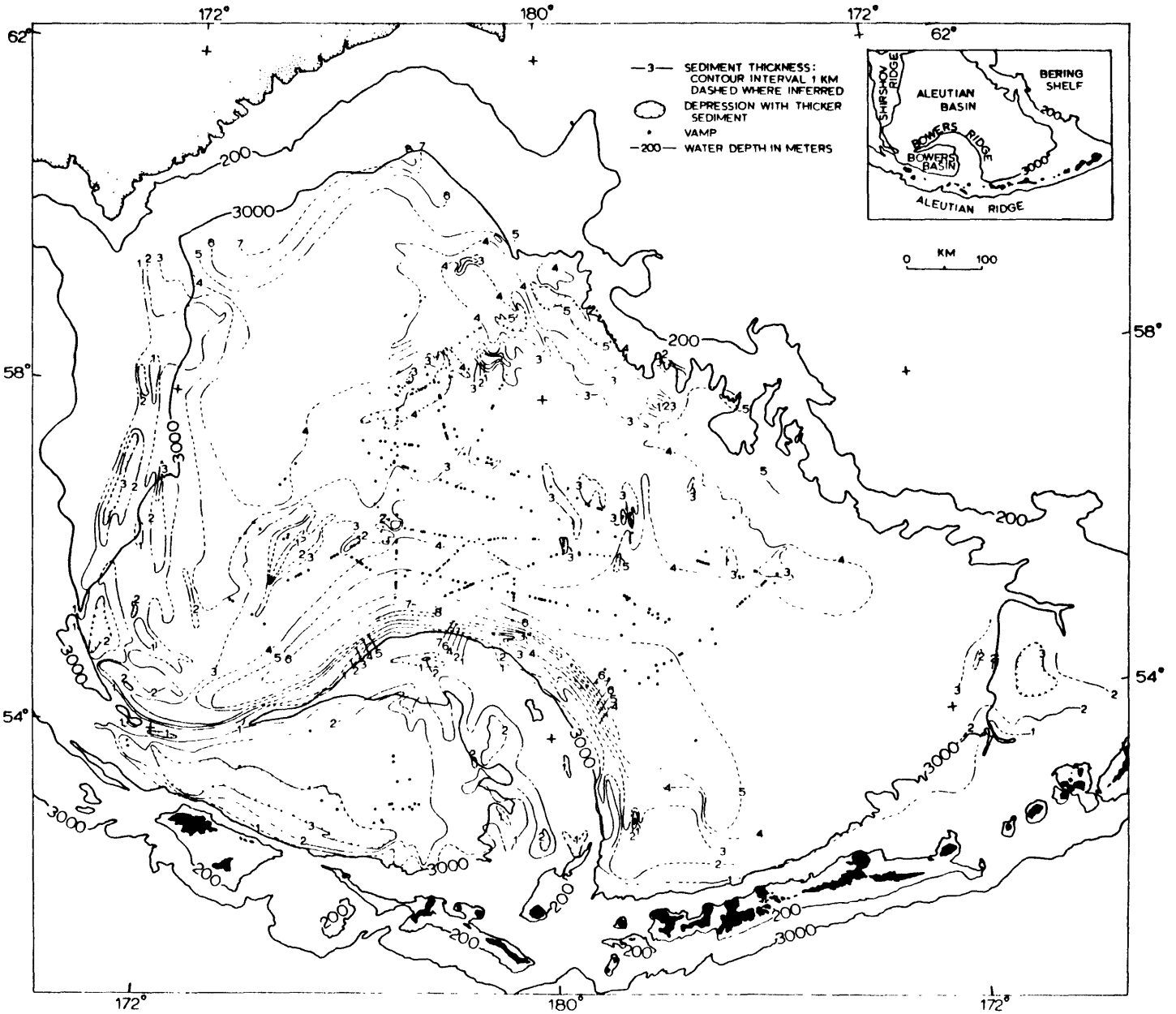

Figure 11. Isopach map showing total thickness of sedimentary rocks overlying acoustic basement (update from Cooper and others; 1977a). Black dots show location of VAMP's. Since the seafloor of the abyssal basin area is nearly flat, the topographic relief implied by the contours is the relief on acoustic basement. Note that many VAMP's are associated with basement topography, yet others are not.

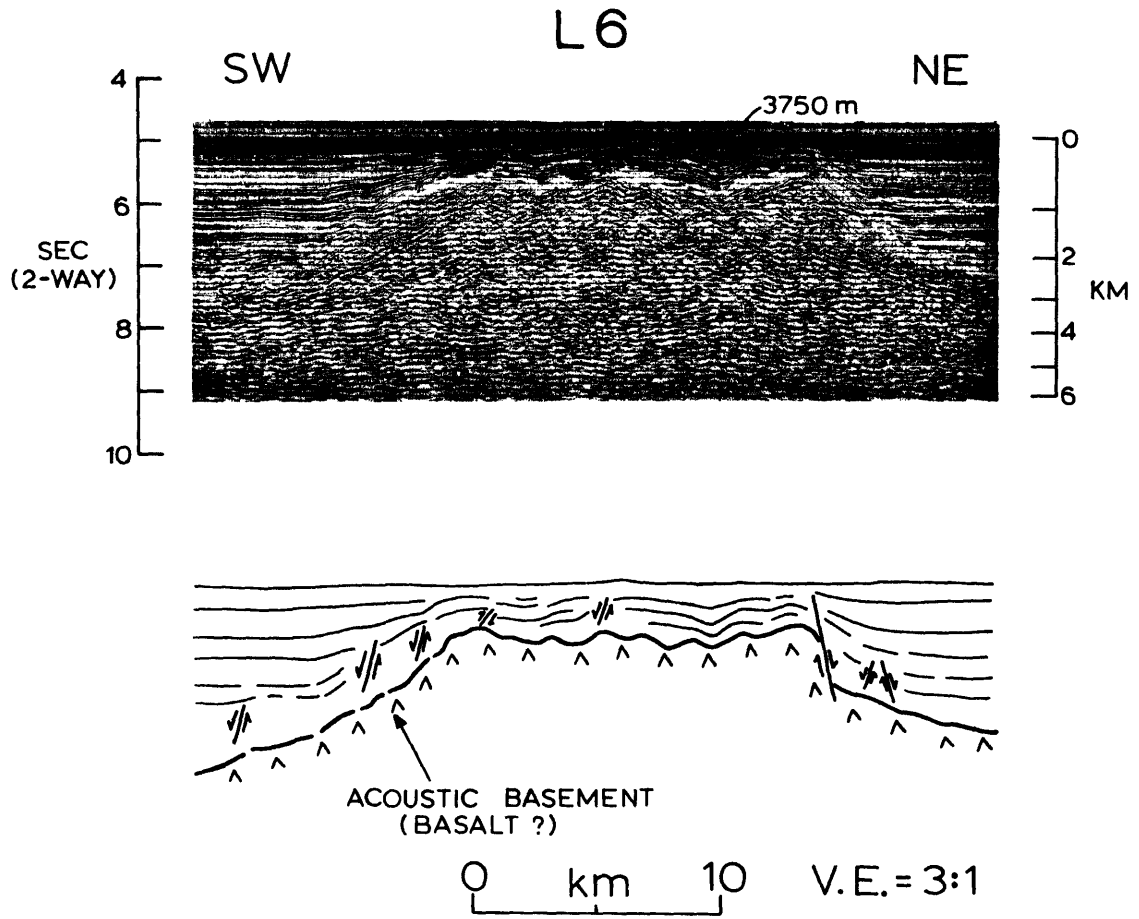

Figure 12. A migrated multichannel seismic reflection profile (L6) along the axis of Sounder ridge; see Figure 7 for location. The ridge has a relief of about 3 km. Sedimentary layers that cover the ridge are folded, faulted, and upbowed to form a set of low-relief sea-floor ridges. Depth scale from Cooper and others (1977a).

Thermal and Sedimentation History

Schlanger and Combs (1975) indicate that the hydrocarbon potential of a mature basin, such as the Aleutian Basin, is largely dependent upon the length of time that its sedimentary section has been exposed to the high burial temperatures necessary for the kerogen-hydrocarbon transformation. If curves for temperature versus age and depth for known oil and gas producing basins (Schlanger and Combs, 1975, Figs. 10, 11) are applied to the Aleutian Basin, the generation of hydrocarbons could occur in horizons as young as early Miocene (18 to 23 m.y.). Although the observed heat flow values in the Aleutian Basin are not high, the average heat flow (1.44 ± 0.22 ucal/cm^{2}sec; Watanabe and others, 1977) and the thermal conductivity of the sediment (2.5 mcal/cm-sec-^{o}C, Erickson, 1973) give a thermal gradient (58^{o}/km) that is sufficient to reach the onset of hydrocarbon generation (50-100^{o}C) at relatively shallow sub-bottom depths (0.9-1.8 km). The sedimentation rate measured at DSDP site 190 in the western Aleutian Basin is high, about 100 m/m.y from Holocene to upper Miocene time (Creager and Scholl and others, 1973). Consequently, the actual heat flow values and associated temperature gradients, after correction for sedimentation effects, may be 10-25% larger than observed. Locally higher heat flow valves or higher sedimentation rates would both cause maturation temperatures to occur at shallower sub-bottom depths. Because the sediment thickness in the Aleutian Basin ranges from 2 to 9 km (Fig. 5), temperatures suitable for biogenic and thermogenic degradation of organic matter (50 - 100^{o}C) may be found throughout the basin.

Organic Carbon-Hydrocarbons

DSDP holes within the Aleutian and Bowers Basins (Sites 188, 189, 190)

are the sole source of sub-seafloor information concerning the organic carbon and hydrocarbon content of sediment underlying the abyssal basins. The maximum sub-bottom penetration, 871 meters, is at site 189. Organic carbon values for the diatomaceous silty clay and mudstone (Holocene to middle Miocene age) sampled at the three DSDP holes are nearly uniform with depth and range from 0.2% to 0.8% (Bode, 1973); the average is 0.42 + 0.15% for 50 samples. Late Cenozoic sedimentary rocks cored (Gershanovich, 1968) and dredged (Marlow and others, 1976; Underwood and others, 1979) from the northern and eastern Bering Sea continental margin have a similar organic carbon content.

Organic gases in the abyssal basin sediment have been measured both in surface samples from the Aleutian Basin and in sub-surface cores at DSDP holes 185, 189, and 191. The surface samples were collected and analyzed aboard the vessel SEA SOUNDER in June 1977. Gas chromatography on water samples extacted from fresh, two-meter gravity cores shows that only small amounts of gas are present, the gas is totally dissolved in the interstital water (no free gas bubbles), and the primary constituent is methane. A compilation of the gas analyses (Fig. 13) indicates that the methane concentration increases with sub-bottom depth at all sites. Generally, those sites (Sta. 2, 3, 6) located in areas where VAMP's are abundant (see Fig. 11) have higher methane concentrations at comparable sub-bottom depths than those sites lying either at the edge (Sta. 1, 4) or outside (Sta. 8, 9) of the zone of VAMP's. Interestingly, the highest concentration of methane is found directly over a VAMP (Sta. 2; Fig. 13) that is associated with a buried basement ridge (BS 1, Fig. 10). Gases in sediment cores recovered at DSDP drilling sites are also primarily methane, although ethane is present at site 189 near the base of the

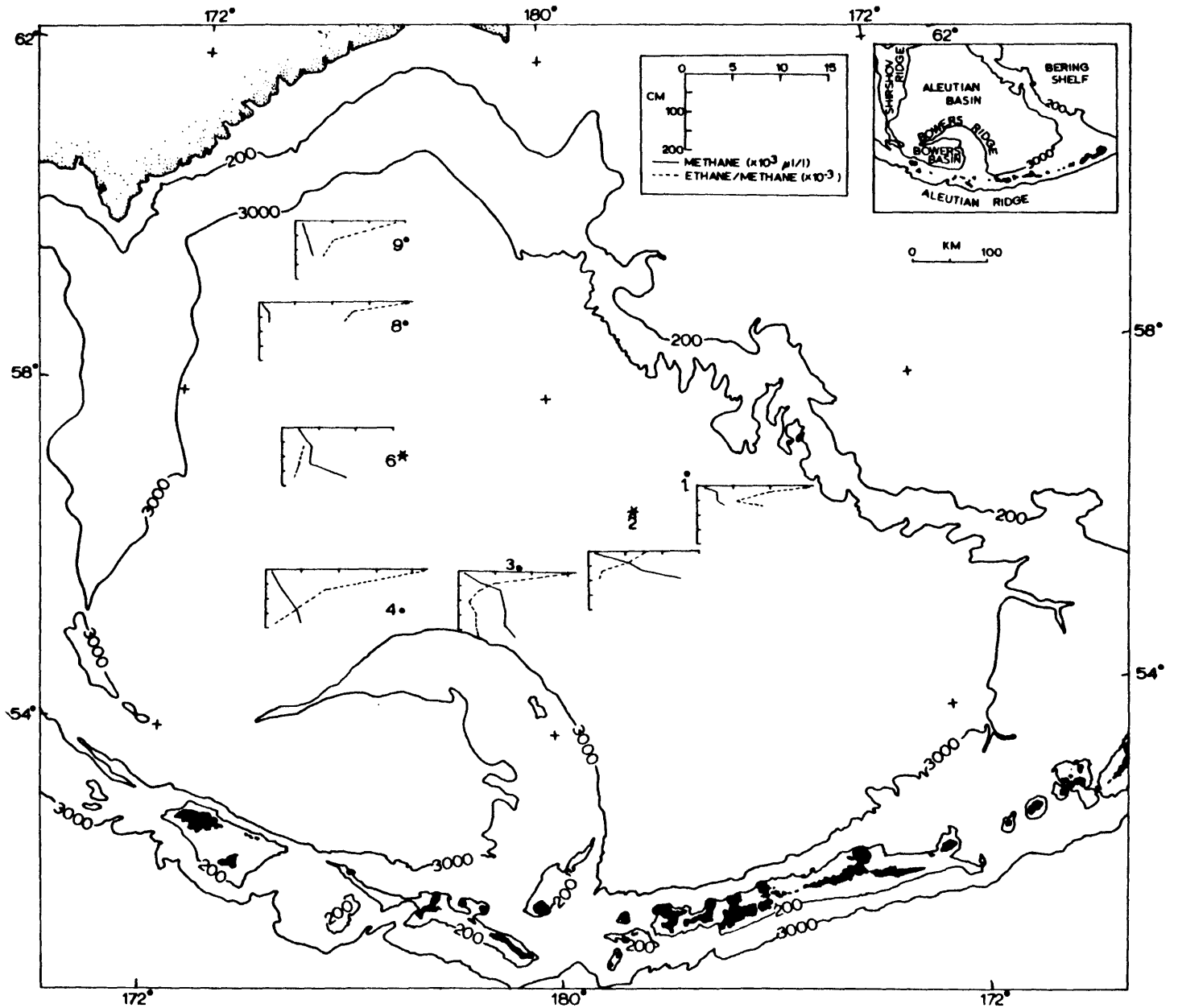

Figure 13. Concentration of hydrocarbon gases measured in fresh gravity core samples collected during June 1977. Stations 2 and 6, shown by stars, are located directly over the top of the VAMP's illustrated in Figures 9 and 10, respectively. Graphs show both the total methane concentration and the ethane/methane ratio in the upper 2 meters beneath the seafloor. Methane concentrations are small, they increase with depth, and they are larger in the area of VAMP's (see also Figures 9, 11).

Aleutian Ridge (McIver, 1973; Claypool and others, 1973).

The origin of the organic gases in both surface and subsurface samples could be the result either of bacteriological fermentation or of thermal degradation of organic compounds. Carbon-isotope measurements for the methane gases recovered at DSDP sites close to the Aleutian Basin (sites 185, 189, 191) are relatively small (C 13 = - $70^{o}/00$; Claypool and others, 1973), suggesting a biogenic source. Similar isotope measurements could not be made on the surface gas samples because the quantity of gas in the surface cores was too small. The paucity of the higher hydrocarbon fractions in the surface gases also favors a biogenic origin for the methane but does not exclude a thermogenic origin. At site 189, the amount of ethane increases with depth, and like other DSDP sites in the Bering Sea area (186, 191), the absolute concentration of ethane shows a positive correlation with the inferred temperature flux; sites with higher heat flow generally have larger ethane concentrations at the same depth (Claypool and others, 1973, Figure 9). The origin of the ethane at these sites is thermogenic, and the ethane could be coming either from in situ generation along the natural geothermal gradient or from upward migration out of an existing hydrocarbon reservoir (Claypool and others; 1973). Organic gas measurements were not made at DSDP site 190 within the Aleutian Basin, therefore we do not know if higher hydrocarbon fractions are present at depth near an area that has a concentration of VAMP's.

Low-surface concentration of gas, even over potential gas pockets (VAMP's), suggest that if gases are accumulating at depth, they are not diffusing through the overlying sediment and are not reaching the surface in significant quantities. The multi-channel data recorded over a VAMP (V2, Fig. 9), which has been cored and analysed for surface gases (Sta. 6, Fig. 13),

show that the reflectors between the top of the VAMP and the seafloor are discontinuous and phase inverted ("D". Fig. 9). These distributed reflectors suggest that larger concentrations of gas than measured in the upper two meters beneath the seafloor may be present at shallow sub-surface depths.

Potential Reservoir Beds

Subsurface porosity and permeability values have been determined for a small number of core samples recovered from DSDP sites 190 and 188 (Fig. 8A, 8B; Table 3). These two sites are located in different physiographic areas of the deep-water Bering Sea basin , yet the stratigraphic sequences drilled at both sites contain diatomaceous sedimentary beds that may be potential reservoir units. Site 190 lies on the western edge of the Aleutian Basin above a buried basement knoll where the sedimentary sequence is shallower and thinner than in the surrounding basin area. The depositional regime and physical properties (porosity and permeability) at site 190 may differ from those elsewhere in the central Aleutian Basin (zone of VAMP's) because the drilling site is over the knoll. These differences may be small, however, since the acoustic stratigraphy is laterally continuous from site 190 to the center of the basin. Site 188 lies at the perimeter of Bowers Basin on the west flank of Bowers Ridge; the seafloor here is several hundred meters above the basin floor. The sedimentary section at site 188 comprises diatom ooze that has a smaller terrigenous silt and clay component than found at site 190. The porosity and permeability data from site 188 may also be applicable to the central Aleutian Basin where similar oozes are thought to occur.

In general, the porosity of the diatomaceous sediment recovered at Bering Sea drilling sites increases with increasing amounts of diatomaceous debris in

TABLE 3: Permeability and Porosity

Site	Core	Section	Interval Cm	Sub-Bottom Depth Meters	Permeability 1/ MDarcy	Porosity 2/ %	Sediment Type 3/
190	10	1	134-136	151	6	75	Silty diatom ooze
	10	3	119-121	154	16	60	Clay rich silty diatom ooze
	11	4	110-112	202	187	61	Diatom rich silty clay
	11	2	93-95	199	19	82	Silt and clay bearing diatom ooze
	12	2	62-64	227	21		Silt bearing clayey diatom ooze
	12	4	59-61	230	49	64	Silt bearing diatom rich clay
	13	2	39-41	329	25	55	Silt and clay bearing diatom ooze
	13	3	61-63	331	8		Silt and clay bearing diatom ooze
	14	2	42-44	423	19	73	Silt bearing diatomaceous clay
	14	5	114-116	428	33	74	Silt bearing diatomaceous clay
	15	1	86-88	610	37	*69	Clayey diatom ooze
	15	1	114-116	610	24		Clayey diatom ooze
188	8	6	119-121	235	12	81	Diatom ooze
	9	3	99-101	287	18	79	Clay and/or silt bearing diatom ooze
	11	1	128-130	331	22	*63	Silt bearing diatom ooze
	12	1	76-78	425	32	*65	Clay bearing, silty rich diatom ooze
	13	1	137-140	528	13	*55	Silt and clay rich diatom ooze
	14	1	114-117	565	27		Silt rich diatom ooze
	15	2	94-96	575	35	*58	Clay bearing silt rich diatom ooze
	17	1	128-131	602	<0.01	*33	Black mudstone

1/ Permeability measurements made by Core Labs Inc. See Appendix I.

2/ Porosity values determined from shipboard GRAPE density measurements (Creager and others, 1973) using a grain density of 2.5 gm/cc. *Values measured by Core Labs Inc. in January 1979.

3/ Lithologic descriptions from DSDP site reports (Creager and others, 1973).

the sediment (Creager, Scholl and others, 1973; Figs. 14a,b). Compressibility studies on the Bering Sea sediment (Lee, 1973) show that the porosity of diatomaceous ooze (<50% diatom content) does not decrease significantly with increasing burial depths. As the detrital silt and clay component increases (diatom content decreases), however, the sediment becvomes more compressible and the porosity decreases with depth. The range in porosity values is nearly identical (58%-85%) for the diatomaceous sections drilled at sites 190 and 188, however, the scatter in the values for the individual 9-meter cores is different (Figs. 14a,b). At site 188, where the diatom concentrations are high, the correlation between diatom content and porosity is good and the scatter of porosity values is low ($\pm$ 5%). Conversely, at site 190, where the diatom concentrations are lower (30-70%), the diatom-porosity correlation is less apparent and the scatter in porosities is higher ($\pm$ 9%).

Only a small number of permeability measurements have been made at both sites but these values appear to increase with increasing depth (Figs. 14a,b). At site 190, the permeability of the diatomaceous sediment increases from about 10 millidarcys at 150 meters to about 30 millidarcys at 600 meters. Similar values at equivalent depths are observed at site 188. At depths where permeabilities increase, the visual estimates of diatom content decrease (Figs. 14a,b). The decrease (300-600 meters sub-bottom) is more apparent at site 188 than site 190. This apparent correlation between permeability and diatom content is weak because of the unknown error in the visual diatom estimates made onboard ship. Stosur and David (1976), in their work on the diatomite formation of the Lost Hills field, California, have noted that the purer the diatomite, the lower the permeability and the higher

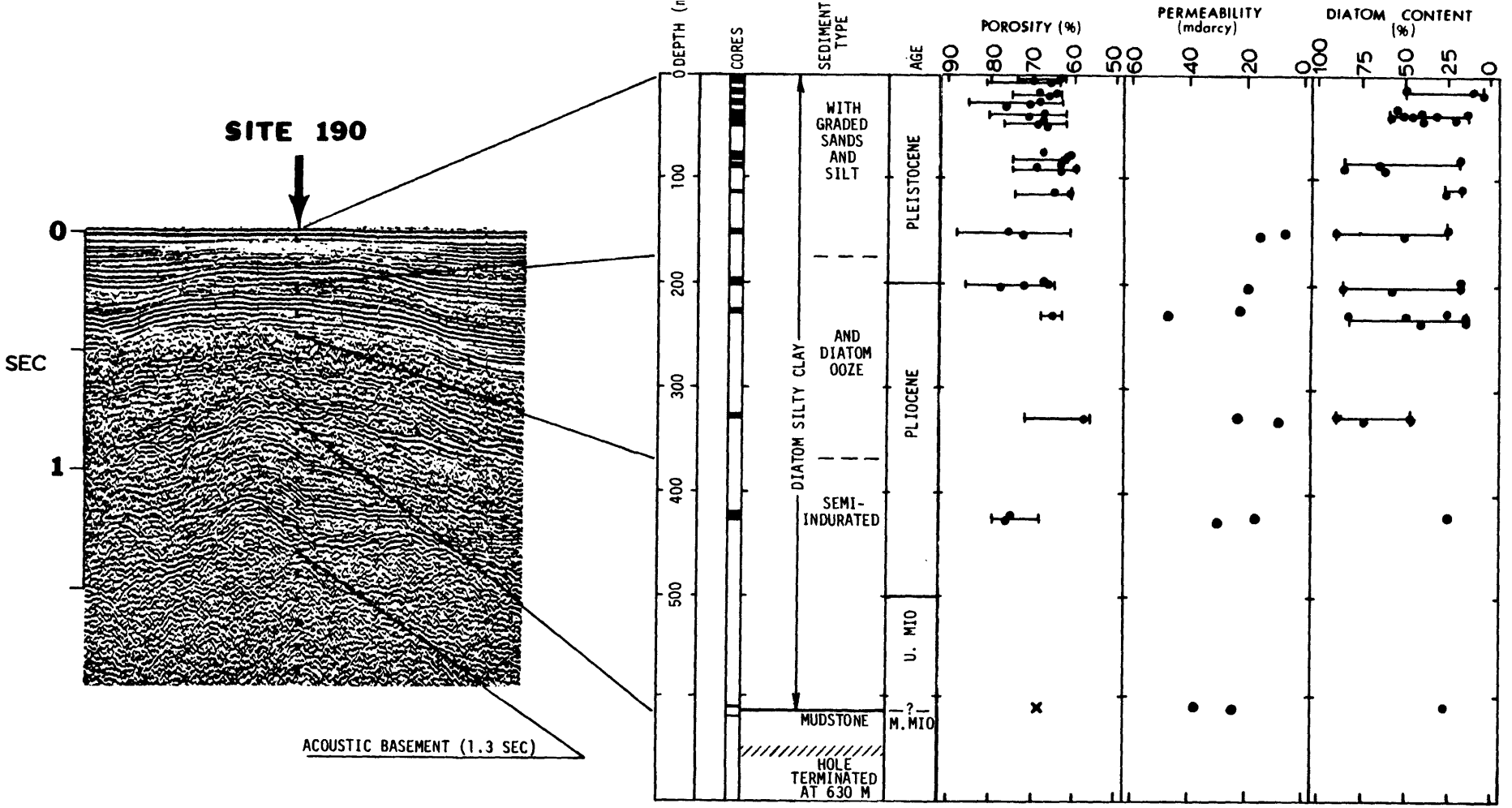

Figures 14a and 14b. Summary of drilling results from DSDP sites 190 and 188 in the Bering Sea modified from Creager, Scholl and others (1973). See Figure 7 for location. Note that above the mudstone (600 meters) the porosities are high and the permeabilities increase with depth. At the mudstone interface the porosity and permeability values drop sharply. Notations used: POROSITY: dots are shore lab measurements (Lee, 1973), bars give the range of shipboard GRAPE porosity determinations (assumed grain density=2.5 gm/cc) for individual 9-meter cores (Creager, Scholl and others, 1973), crosses are 1979 measurements (Table 3); PERMEABILITY: dots are 1979 measurements (Table 3); DIATOM CONTENT: dots are values estimated onboard ship (Creager, Scholl and others, 1973), and bars show the maximum range of the shipboard estimates. Age boundaries are from diatom stratigraphy of Koizumi (1977).

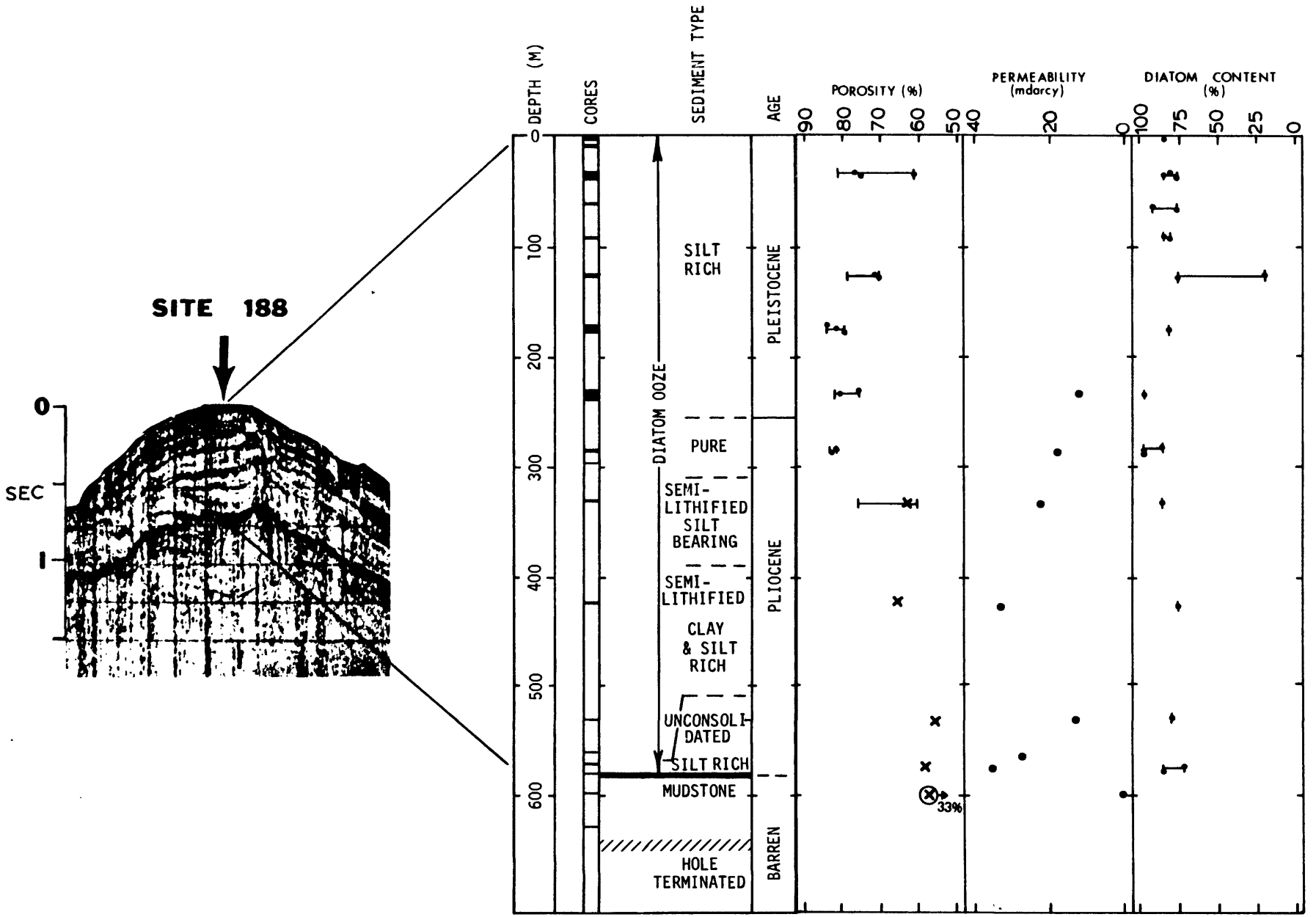
SITE 188
0
SEC
1
DEPTH (M)
CORES
SEDIMENT TYPE
AGE
POROSITY (%)
PERMEABILITY (mdarcy)
DIATOM CONTENT (%)
0
100
200
300
400
500
600
90
80
70
60
50
40
20
0
100
75
50
25
0
SILT RICH
PURE
SEMI-LITHIFIED SILT BEARING
SEMI-LITHIFIED CLAY & SILT RICH
UNCONSOLIDATED SILT RICH
MUDSTONE
HOLE TERMINATED
DIATOM OOZE
PLEISTOCENE
PLIOCENE
BARREN
33%

Figure 14b.

the porosity. They believe high capillary pressure in the diatoms inhibits fluid motion and thereby causes lower permeability for purer diatomite. The correlation observed by Stosur and David (1976) is similar to that which apparently exists at sites 188 and 190. Other investigators, working in the siliceous shales of the Monterey Formation of California, find, however, that the permeability increases with increasing porosity (Larry Beyer, written communication, 1979). The explanation for the downward increase in permeability in the Bering Sea is unclear, yet we suspect that this increase is related to the diatom stratigraphy of the sedimentary section.

The high porosity (60-80%) and good permeability (10-30 millidarcys) of the upper 600 meters of the sediment sections at sites 190 and 188 mark these upper diatomaceous sequences as potential reservoir units for the accumulation of hydrocarbons.

The lower boundary of the potential reservoir units may be controlled by a diagenetic boundary that separates the overlying diatomaceous sediment from underlying indurated mudstone. Beneath most of the Aleutian Basin, the top of the mudstone unit is a prominent refracting horizon that occurs at a sub-bottom depth of about 1 km. At site 190 the boundary is an unconformity associated with a thinned sedimentary section that overlies a buries basement knoll. The unconformity probably does not exist where thicker sedimentary sequences underlie the basin floor. A similar diagenetic boundary has been encountered at most Bering Sea DSDP sites (Hein and others, 1978), and, at site 185, the boundary is associated with higher than typical levels of methane gas (Creager, Scholl, and others, 1973).

The diagenetic boundary is marked by a distinct decrease in both porosity and permeability values (Lee, 1973; Table 3). Hein and others, (1978)

indicate that the boundary results from the dissolution of biogenic silica (opal-A) and the reprecipitation of crystalline silica (opal-CT). Porosity and permeability values have not been determined for the mudstone at site 190; however, at site 188, the porosity drops from 58% to 32% and the permeability decreases from 35 to 0.1 millidarcy across the diagenetic boundary (Figs. 14a,b); Table 3). A drop in porosity across the boundary from 75% to 40% is noted by Lee (1973) at site 185. The lateral continuity of the diagentically altered mudstone unit in the Aleutian Basin may regionally restrict the upward migration of deeply buried thermocatalytic hydrocarbons. Acoustic evidence, such as the observed increase in velocity pull-down with increasing depth beneath some VAMP's, indicates, however, that low velocity pockets may occur deep within the mudstone unit. Possibly these pockets imply that fracture porosity and permeability near VAMP's may allow the upward migration of hydrocarbons into overlying diatomaceous units.

Two lines of evidence suggest that laterally extensive reservoir seals may exist in the Aleutian Basin. At site 190, the lowest permeability values are measured within the turbidite-bearing sequence (0-175) where the diatom content is lowest (clay/silt content highest). The large variation in the fine-grained clay/silt content of the cores in the turbidite sequence indicates that thin, but unsampled, units of impermeable material may exist. The seismic reflection data provide additional evidence relevant to reservoir seals. Multichannel seismic data reveal that a laterally continuous sequence of "railroad track" reflectors underlies the seafloor to a sub-bottom time of 0.5 sec. At this depth, the localized high-amplitude reflections that mark the top of VAMP's appear as narrow disruptions along a continuous reflection horizon. The lateral disruptions can be seen over a horizontal distance of

200-250 km. Other VAMP's that are recorded in the seismic data from different parts of the basin also have their tops near this horizon. Traced to DSDP site 190, the horizon is found to lie near the base of the turbidite-bearing unit. If, as we have speculated, gas or other hydrocarbons have accumulated below this horizon, then a seal at a sub-bottom depth near 0.5 sec has regionally formed in the upper part of the central basins sedimentary section.

A simple model that explains the acoustic configuration of VAMP's and that is based on the porosities and permeabilities measured at site 190 and 188 is illustrated in Figure 15. In the model, the diatomaceous sediment is the primary reservoir unit that contains pockets of low velocity material (LVM). This reservoir unit is sandwiched between an overlying turbidite-bearing unit and an underlying diagenetically altered mudstone unit. The pockets of low velocity material at the top of the VAMP's and within the reservoir are marked by the high-amplitude phase-inverted reflectors and small velocity pull-downs. A more pronounced velocity pull-down (more low velocity material) occurs at greater sub-bottom depths near the mudstone boundary, and typically continues to increase for a few hundred meters beneath the boundary.

An interesting stratigraphic analog of the Bering Sea may be found in the Sea of Japan. The sedimentary section at site 190 is similar to ones drilled in the abyssal part of the Sea of Japan (sites 299, 301; Ingle, Karig and others, 1975). At sites 299 and 301, ethane gas occurs at a sub-bottom depth of 500 meters near the base of a turbidite section that overlies diatomaceous sediment. The diatomaceous beds appear to be the reservoir units for the gas, which is inhibited from migrating upward by the capping, less permeable turbidites. The large quantity of ethane gas found near the base of the turbidites forced a termination of drilling operations. Unlike the Bering

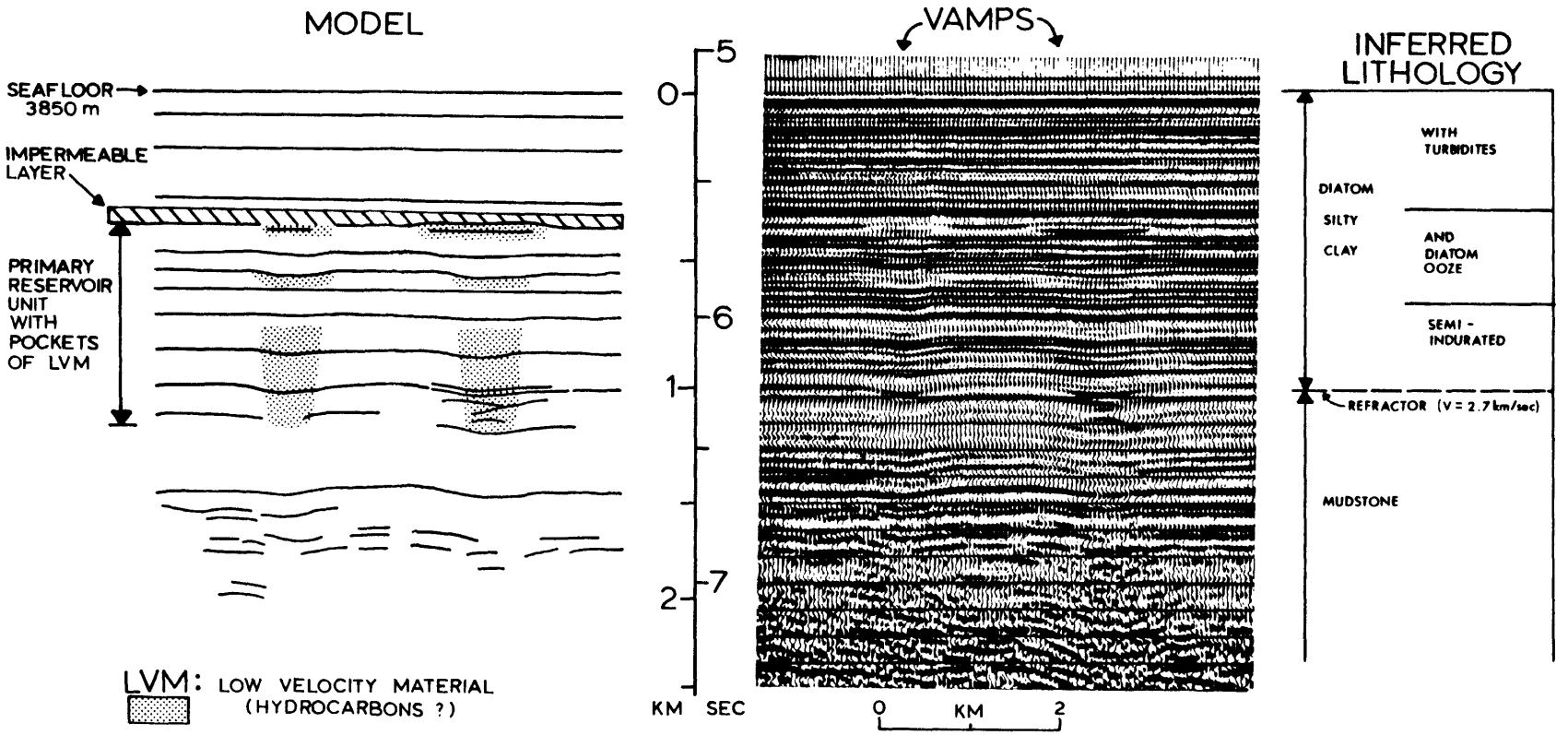

Figure 15. Simple model for explaining VAMP's in terms of lithology, and physical property measurements from DSDP site 190. See Figure 7 for location. The reservoir unit is the diatomaceous sediment that is sealed by overlying turbidites and is underlain by indurated mudstone. High-amplitude, phase-inverted reflectors with underlying velocity pull-downs are found within the VAMP's and are caused by pockets of low-velocity material, possibly gas or other hydrocarbons. Depth scale from Cooper and others (1977a).

Sea, VAMP's have not been reported from the Sea of Japan.

CONCLUSIONS

The Navarin basin province is a recently discovered frontier shelf area of significant hydrocarbon potential. Though relatively unexplored and unknown, the province underlies at least 45,000 km^2 (11 million acres) of the shelf and comprises three large basins. The sedimentary sequences filling the basins are 10 to 15 km thick. Although Cretaceous units may form part of the stratified sequences, most of the section is probably of Cenozoic age.

Reconnaissance geophysical data reveal anticlinal or diapiric(?) structures, stratigraphic pinchouts, and growth faults within the basins. Discoveries of oil and gas in Tertiary beds in nearby Siberia encourage speculations that hydrocarbon deposits occur in the Navarin basins. The vast size of these basins statistically argues for the presence of oil and gas beneath the northwestern Bering Sea shelf.

Further exploration of the Navarin basins and the adjacent continental slope is needed. Seismic-reflection, and seismic-refraction surveys, as well as gravity and magnetic data are especially needed to understand the geologic history of these large structures. Samples obtained by dredging on the continental slope and by direct drilling in the basins may confirm the existence of suitable source and reservoir beds within the Navarin province.

The presence, or absence, of economically significant hydrocarbon accumulations in marginal basins of the Pacific, such as the Bering Sea Basin, is unknown, primarily because little exploratory work has been attempted. The extreme water depths (3,000-4,000m) pose severe technical problems for exploration as well as possible production activities. Exploratory programs

in these areas have, therefore, been limited to regional reconnaissance surveys. Since 1974, energy resource investigations in the Aleutain Basin by the U.S. Geological Survey have identified several intrabasin features which, we believe, suggest that the basin may be the habitat for significant accumulations of gas and possibly other hydrocarbon products.

Perhaps the best evidence for these deposits, in the absence of deep subsurface hydrocarbon measurements, is the widespread occurrence of VAMP's. The general acoustic character of deep-water VAMP's (phase inverted, high amplitude reflector underlain by a velocity pulldown) is similar to that of some "bright spots" discovered in hydrocarbon producing areas on the continental shelf. The question of what hydrocarbons, if any, are present and are causing these acoustic features (VAMP's) cannot be answered without drilling information in the central Aleutian Basin. On the basis of limited subsurface information that includes an analysis of gases in shallow sediment from the Aleutian Basin (Fig. 13) and topical studies on DSDP cores from surrounding areas (Creager, Scholl and others, 1973) the likely cause of the VAMP's is the presence of low velocity pockets of biogenic methane gas. The gas appears to be trapped within porous diatomaceous sediment that is sandwiched between underlying indurated mudstone and shallow turbidite unit.

Other higher order hydrocarbons originating from greater depths may also be present, however. A common characteristic of VAMP's that is difficult to explain unless there is additional low velocity material, presumably hydrocarbon charged deposits beneath the VAMP's, is the increase in the velocity pulldown with depth that commences near the top of the mudstone unit (Fig. 15). These hydrocarbons, if present, could be migrating upward from either in situ generation points or deep seated reservoirs. The association

of VAMP's with basement relief (Figs. 10 and 11) allows the existence of the deep structural pathways along which thermogenic hydrocarbons could move upward from the mudstone into the diatomaceous reservoir rocks. Temperature gradients within the sedimentary section are sufficiently large to allow in situ generation of thermogenic hydrocarbons at moderate depths (2-4 km) if suitable organic material is present within the mudstone unit.

Figure 16 summarizes three important factors for evaluating the hydrocarbnon potential of the Aleutian Basin, namely the areas of thick sediment, large basement relief, and VAMP concentrations. Interestingly, the area in which VAMP's are found generally corresponds with the areas of thinner sediment (less than 4 km thick) and larger basement relief (greater than 1 km). The same area may also have large methane concentrations in the surface sediments (Fig. 13) and slightly higher heat flow values (higher sub-seafloor temperatures; Cooper and others, 1977c). In addition, the central basin is characterized by long-wavelength magnetic lows that are recorded in both satellite and shipboard measurements (Fig. 17). The unusual inverse correlation of negative (rather than positive) magnetic anomalies with shallow igneous basement beneath the thin sediments suggests that the sub-crustal heating and demagnetizing processes proposed by Cooper and others, 1977c, may be affecting this area. If thermogenic hydrocarbons are present in VAMP's, they may be the manifestation of the regional thermal event that may have effected the central part of the basin.

The general uniformity in the geology and geophysics of the sedimentary section in the central part of the Aleutain Basin, where these regional correlations are observed, suggests that if hydrocarbon accumulations of economic importance can be substantiated for one locality in this region, then

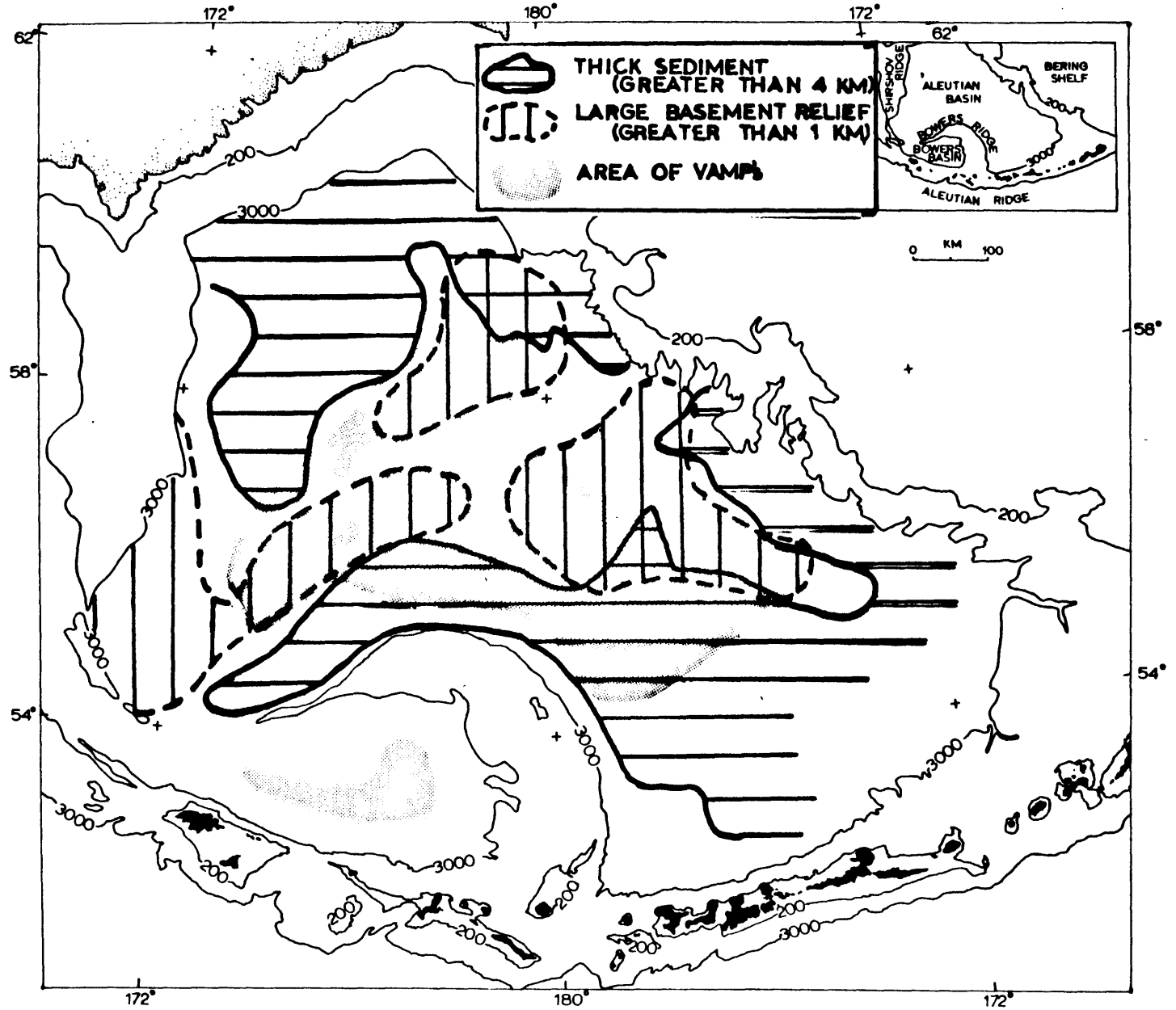

Figure 16. Summary map showing areas of thick sediment, large basement relief, and VAMP concentrations in the abyssal basin areas, compiled from Figure 11. Note that the central and eastern parts of the Aleutian Basin are generally associated with thinner sediments, larger basement relief, and more VAMP's than other parts of the basin; these areas are perhaps the best prospective ones for potential hydrocarbon accumulations.

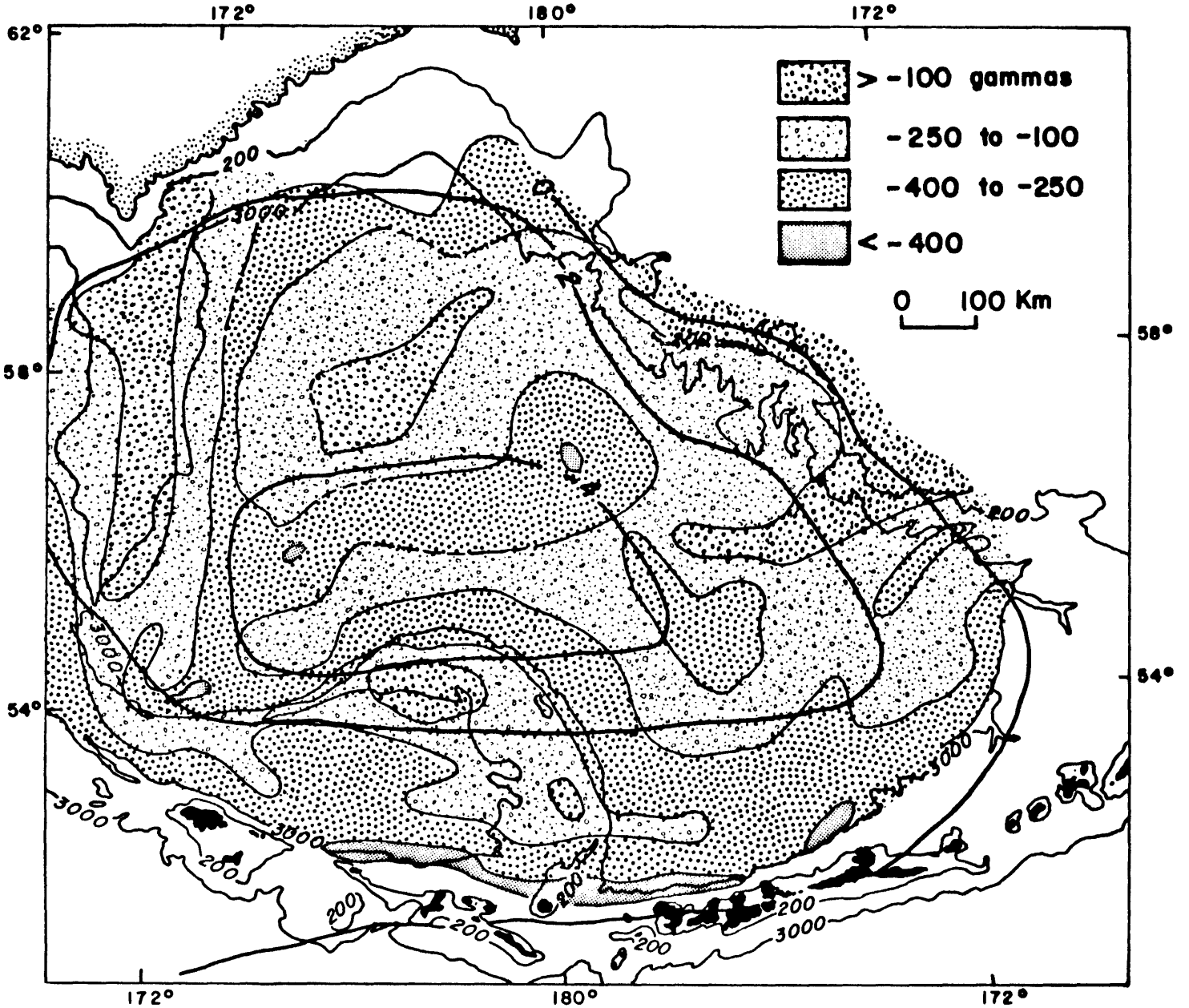

Figure 17. Map of long-wavelength (greater than 100-150 km) magnetic anomalies recorded in both shipboard and satellite data (from Cooper and others 1977c). Note the broad negative anomalies that lie in the central Aleutian Basin; these anomalies are generally located over areas that have shallow basement with large vertical relief (compare with Figure 16). This inverse correlation may result from sub-crustal heating and demagnetization. Shipboard magnetics are the stippled pattern and satellite data are the heavy contours.

it is likely that similar deposits may be found throughout the entire are. The most promising economic area of the Aleutian Basin, the area of VAMP's is large (about the size of the state of Washington) and the area lies on the American side of the international treaty line. Although we can only speculate on the future economic value, if any, of this deep-water 'frontier area, our data indicate that the basin is nonetheless a promising one and therefore deserves further exploration for energy resources.

In summary, the hydrocarbon prospects of the Navarin basin province as well as the adjacent Aleutian Basin are both good. Because both areas are very remote, development of these areas may not take place for a number of years.

REFERENCES

Anonymous, 1977, Descriptions of ocean sediment cores, In Announcement of availability of marine geology data: U.S. Dept. of Commerce, Natl. Oceanic and Atmospheric Admin., Environmental Data Serv. Natl. Geophys. and Solar-Terrestrial Data Center (D62), Boulder, CO 80302.

Beikman, H., 1974, Preliminary geologic map of the southwest quadrant of Alaska: U.S. Geol. Survey Misc. Field Studies Map MF-611, 2 sheets, scale 1:200,000.

Beikman, H., 1978, Preliminary geologic map of Alaska: U.S. Geol. Survey Map, 2 sheets, scale 1:2,500,000.

Bode, G.W., 1973, Carbon-Carbonate, In Creager, J.S., ed., et al., Initial reports of the Deep Sea Drilling Project, v. 19: Washington, D.C., U.S. Govt. Printing Office, p. 662-666.

Burk, C.A., 1965, Geology of the Alaska Peninsula Island arc and continental margin: Geol. Soc. America Mem. 99, 250 p.

Burlin, Yu. K., and Arkhipov, A. Ya., 1973, Oil-gas basins of the east of the USSR: International Geology Review, v. 17, no. 10, p. 1201-1206.

Childs, J.R., and Cooper, A.K., 1979, Marine seismic sonobuoy data from the Bering Sea region: U.S. Geol. Survey Open-File Rept. 79-371.

Claypool, G.E., Presley, B.J., and Kaplan, I.R., 1973, Gas analyses in sediment samples from Legs 10, 11, 13, 14, 15, 18, 19, in Creager, J.S., ed., and others, Initial reports of the Deep Sea Drilling Projects, v. 19: Washington, D.C., U.S. Govt. Printing Office, p. 879-884.

Cooper, A.K., 1977, Marine geophysical investigations in the Bering Sea Basin: U.S. Geol. Survey Circ. 751-B, p. 98-100.

Cooper, A.K., and Scholl, D.W., 1974, Regional crustal inhomogeneities - Bering Sea marginal basin (abs.): EOS (Am. Geophys. Union Trans.), v. 55, p. 1187.

Cooper, A.K., Bailey, K.A., Howell, J., Marlow, M.S., and Scholl, D.W., 1976a, Preliminary residual magnetic map of the Bering Sea Basin and Kamchatka Peninsula: U.S. Geol. Survey Misc. Field Studies Map MF-715, scale 1:2,500,000.

Cooper, A.K., Scholl, D.W., and Marlow, M.S., 1976b, Mesozoic magnetic lineations in the Bering Sea marginal basin: Jour. Geophys. Research, v. 81, p. 1916-1934.

Cooper, A.K., Scholl, D.W., and Marlow, M.S., 1976c, A plate tectonic model for the evolution of the eastern Bering Sea Basin: Geol. Soc. America Bull., v. 87, p. 1119-1126.

Cooper, A.K., Childs, J.R., Marlow, M.S., Rabinowitz, R.D., Scholl, D.W., and Ludwig, W.J., 1977a, Preliminary isopach and structure contour maps of the Bering Sea Basin: U.S. Geol. Survey Misc. Field Studies map MF-907.

Cooper, A.K., Childs, J.R., Marlow, M.S., and Scholl, D.W., 1977b, Multichannel seismic reflection data in the Bering Sea Basin (abs.): Geol. Soc. America program, Annual Mtg., Sept. 1977, p. 934.

Cooper, A.K., Marlow, M.S., and Scholl, D.W., 1977c, The Bering Sea - A multifarious marginal basin, In: Island arcs, deep sea trenches, and back-arc basins, v. 1: Am. Geophys. Union, p. 437-450.

Cooper, A.K., Scholl, D.W., Marlow, M.S., Childs, J.R., Redden, G., and Kvenvolden K., 1978, The Aleutian Basin, Bering Sea--a frontier area for hydrocarbon exploration: Offshore Technology Conf. Proc., May 1978, p. 353-371.

Cooper, A.K., Marlow, M.S., and Scholl, D.W., 1979, Thick sediment accumulations beneath continental margin of outer Bering Sea (abs): AAPG-SEPM program, Annual Convention, April 1979, p. 72.

Creager, J.S., Scholl, D.W., and others, 1973, Initial reports of the Deep Sea Drilling Project, v. 19: Washington, D.C., U.S. Gov't Printing Office, 193 p.

Erickson, A., 1973, Initial report on downhole temperature and shipboard thermal conductivity measurements, Leg 19, Deep Sea Drilling Project, In: Creager, J.S., ed., and others, Initial reports of the Deep Sea Drilling Project, v. 19: Washington, D.C., U.S. Govt. Printing Office, p. 643-656.

Ewing, M., Ludwig, W.J., and Ewing, J., 1965, Oceanic structural history of the Bering Sea: Jour. Geophys. Research, v. 70, p. 4593-4600.

Foster, T.D., 1962, Heat flow measurements in the northeast Pacific and in the Bering Sea: Jour. Geophys. Research, v. 67, p. 2991-2993.

Frazer, J.Z., Hawkins, D.L., Hydock, L., Crocker, W.L., Schoenbechler, M., Newhouse, D.A., and Chase, T.E., 1972, Surface sediments and topography of the North Pacific; Chart 2: La Jolla, Calif., Scripps Inst. Oceanography, Geol. Data Center, Tech. Rept. Series TR-27.

Gershanovich, D.E., 1968, New data on geomorphology and recent sediments of the Bering Sea and the Gulf of Alaska: Marine Geology, v. 6, p. 281-296.

Gnibidenko, H.S., 1973, Tectonics of the floor of the Bering Sea: Geotectonics, v. 4, p. 237-243.

Hamilton, E.L., Moore, D.G., Buffington, E.C., Sherrer, P.L., and Curray, J.R., 1974, Sediment velocities from sonobuoys: Bay of Bengal, Bering Sea, Japan Sea and North Pacific: Jour. Geophys. Research, v. 79, no. 17, p. 2553-2668.

Hanna, G.D., 1929, Fossil diatoms dredged from Bering Sea: San Diego Nat. Hist. Trans., v. 5, p. 289-296.

Hein, J.R., Scholl, D.W., Barron, J.A., Jones, M.G., and Miller, J., 1978, Diagenesis of late Cenozoic diatomaceous deposits and formation of the bottom simulating reflector in the southern Bering Sea: Sedimentology, v. 25, p. 155-181.

Hopkins, D.M., 1967, The Cenozoic history of Beringia--a synthesis, In: Hopkins, D.M., ed., The Bering Land bridge: Stanford, Calif., Stanford University Press, p. 451-484.

Hopkins, D.M., Scholl, D.W., Addicott, W.O., Pierce, R.L., Smith, P.B., Wolfe, Jr., Gershanovich, D., Kotenev, B., Lohman, K.E., Lipps, J.H., and Obradovich, J., 1969, Cretaceous, Tertiary, and early Pleistocene rocks from the continental margin in the Bering Sea: Geol. Soc. America Bull., v. 80, p. 1471-1486.

Hopkins, D.M., and Scholl, D.W., 1970, Tectonic development of Beringia, late Mesozoic to Holocene (abs.): Bulletin of the American Association of Petroleum Geologists, v. 54, no. 12, p. 2487-2488.

Houtz, R., Ewing, J., and Buhl, P., 1970, Seismic data from sonobuoy stations in the northern and equatorial Pacific: Jour. Geophys. Research, v. 75, p. 5093.

Ingle, J.C., Jr., Karig, D.E., and others, 1975, Initial reports of the Deep Sea Drilling Project, v. 31: Washington, D.C., U.S. Govt. Printing Office, 927 p.

Kienle, J., 1971, Gravity and magnetic measurements over Bowers Ridge and Shirshov Ridge, Bering Sea: Jour. Geophys. Research, v. 76, p. 7138-7153.

Koizumi, I., 1977, Diatom biostratigraphy in the North Pacific Region, In: Chinzei, Ikebe et al. (ed.) in Proc. First Int. Congress on Pacific Neogene, Tokyo, 1976, Kaiyoshyppan Co. Ltd., Tokyo, pp. 235-253.

Lee, H.J., 1973, Measurements and estimates of engineering and other physical properties, leg 19, In: Creager, J.S., ed., and others, Initial reports of the Deep Sea Drilling Project, v. 19: Washington, D.C., U.S. Govt. Printing Office, p. 701-719.

Lisitsyn, A.P., 1966, Protsessy Sovremennogo Osodko' obrazovaniya v Beringovom More: Akad. Nauk SSR Inst. Okeal., Moskva, 574 p. (Recent sedimentation in the Bering Sea: Israel Program for Sci. Translations, 1969, Jerusalem; U.S. Dept. of Commerce, Clearinghouse for Federal Sci. Tech. Info., Springfield, VA, 614 p.)

Ludwig, W.J., 1974, Structure of the Bering Sea basins, In: C.A. Burk and C.L. Darke, eds., The geology of continental margins: New York, Springer, p. 661-668.

Ludwig, W.J., Houtz, R.E., and Ewing, M., 1971a, Sediment distribution in the Bering Sea: Bowers Ridge, Shirshov Ridge, and enclosed basins: Jour. Geophys. Research, v. 76, p. 6367-6375.

Ludwig, W.J., Mavauchi, S., Den, N., Ewing, M., Hatta, H., Houtz, R.E., Yoshii, T., Asanuma, T., Hagiwara, K., Saito, T., and Ando, S., 1971b, Structure of Bowers Ridge, Bering Sea: Jour. Geophys. Research, v. 76, p. 6350-6366.

Marlow, M.S., Scholl, D.W., Cooper,A.K., and Buffington, E.C., 1976, Structure and Evolution of Bering Sea shelf south of St. Lawrence Island, Bulletin of the American Association of Petroleum Geologist, v. 60, no. 2, p. 161-183.

.Marlow, M.S., Cooper, A.K., Scholl, D.W., Vallier, T.L., and McLean, H., 1979a, Description of dredge samples from the Bering Sea continental margin: U.S. Geological Survey Open-File Report 79-1139, 5pp.

Marlow, M.S., Gardner, J.V., Vallier, T.L., McLean, H., Scott, E.W., and Lynch, M.B., 1979b, Resource report for proposed OCS sale No. 70 St. George basin, Alaska: U.S. Geological Survey Open-File Report, in press.

Marlow, Michael S., Scholl, D.W., Cooper, A.K., and Jones, D.L., 1979c, Shallow-water Upper Jurassic rocks dredged from Bering Sea continental margin: American Association of Petroleum Geologists Bull., v. 63, no. 3, 1979c, p. 490-491.

Marlow, M.S., 1979, Hydrocarbon prospects in the Navarin basin province, northwestern Bering Sea shelf: The Oil and Gas Journal, in press.

Marshall, V.B., Cooper, A.K., and Childs, J.R., 1978, Recent Heat Flow Measurements in the Aleutian Basin, Bering Sea (abs.): EOS (Am. Geophys. Union Trans.) v. 59, p. 384.

McIver, R.D., 1973, Hydrocarbons in canned muds from sites 185, 186, 189, 191, In: Creager, J.S., ed., and others, Initial reports of the Deep Sea Drilling Project, v. 19: Washington, D.C., U.S. Govt. Printing Office, p. 875-878.

Oil and Gas Journal, 1977, Russia drilling its deepest Kamchatka test: v. 75, no. 11, p. 23.

Rabinowitz, P.D., and Cooper, A.K., 1977, Structure and sediment distribution in the western Bering Sea basin: Marine Geology, v. 24, p. 309-320.

Regan, R.D., Cain, J.E., and David, W.M., 1975, A global magnetic anomaly map, Jour. Geophys. Research, v. 80, p. 794-802.

Schlanger, S.O., and Combs, J., 1975, Hydrocarbon potential of marginal basins bounded by an island arc: Geology, July, p. 397-400.

Scholl, D.W., Buffington, E.C., and Hopkins, D.M., 1966, Exposure of basement rock on the continental slope of the Bering Sea: Science, v. 153, p. 992-994.

Scholl, D.W., Buffington, E.C., and Marlow, M.S., 1970, Aleutian-Bering Sea region seismic reflection profiles, 1969: U.S. Geological Survey Open-File Report 76-748, 1 pl.

Scholl, D.W., Buffington, E.C., and Marlow, M.S., 1975, Plate tectonics and the structural evolution of the Aleutian-Bering Sea region, In: Forbes, R.B., ed., Contributions to the geology of the Bering Sea Basin and adjacent regions: Geol. Soc. of America Spec. Paper 151, p. 1-32.

Scholl, D.W., Buffington, E.C., Marlow, M.S., 1976. Aleutian-Bering Sea region seismic reflection profiles: U.S. Geol. Survey Open-File Rept. 76-748.

Scholl, D.W., and Cooper, A.K., 1978, VAMP's: Possible hydrocarbon-bearing structures in the Bering Sea Basin: Bull. Amer. Assoc. Petroleum Geologists, v. 62, p. 2481-2488.

Scholl, D.W., And Creager, J.S., 1973, Geologic synthesis of Leg 19 (DSDP) results: Far North Pacific, Aleutian Ridge and Bering Sea, In: Creager, J.S., ed., and others, Initial reports of the Deep Sea Drilling Project, v. 19: Washington, D.C., U.S. Govt. Printing Office, p. 897-913.

Shor, G.G., Jr., 1964, Structure of the Bering Sea and the Aleutian Ridge: Marine Geology, v. 1, p. 213-219.

Soloveva, N.M., Karta Anomalnovo Magnitovo Polya Teritori SSR, Ministerstvo Geologii SSR, 1968.

Stone, D.B., 1968, Geophysics in the Bering Sea and surrounding areas: A review: Tectonophysics, v. 6, p. 433-460.

Stosur, J.J., and David A., 1976, Petrophysical evaluation of the diatomite formation of the Lost Hills field, California: Jour. Petroleum Technology, v. 28, p. 1138-1144.

Underwood, M.B., Vallier, T.L., Gardner, J.V., and Barron, J.A., 1979. Age, grain, size, mineralogy, and carbon/carbonate content of Miocene and Pliocene samples from dredge hauls, DSDP holes 184b and 185, and the Sandy River Well, southern Bering Sea continental margin and Alaska Peninsula: U.S. Geol. Survey Open-File Rept. 79-450.

Vorobev, N.M., 1970, Results of marine magnetic surveys adjacent to the western parts of the Aleutian Island Arc: Acad. Sciences USSR, Siberian Div., Trans. SAXKNII, No. 24, in Russian.

Watanabe, T., Langseth, M.G., and Anderson, R.N., 1977, Heat flow in back-arc basins of the western Pacific, In: Island arcs, deep sea trenches, and back-arc basins, v. 1: Am. Geophys. Union, p. 137-162.

Watts, A.B., 1975, Gravity field of the northwest Pacific Ocean basin and its margin: Aleutian arc-trench system, Geol. Soc. America Map and Chart Services, MC-10.

Yanshin, A.L., ed., 1966, Tectonic map of Eurasia: Geol. Inst. Acad. Sci. USSR Moscow (in Russian), scale 1:5,000,000.

Appendix I - Permeability and porosity measurements

The permeability and porosity values listed in Table I were measured by Core Labs Inc., Bakersfield, California in January 1979 for the U.S. Geological Survey. Since few, if any permeability measurements have been made on semi-consolidated deep-sea sediment, a new procedure had to be designed by Core Labs to handle the DSDP sediment samples.

Permeability:

Transversely-oriented sediment plugs, 1 1/4 inches in diameter by 1 inch long, were extracted from the DSDP cores with a plastic sampling tube. The water-saturated sediment was dried in a humidity oven by decreasing the oven's humidity (100% to 10%) and temperature until all free water was expelled. The drying procedure was done slowly over a period of days to avoid shrinkage of the hydrated clay minerals due to loss of absorbed water. The plugs were mounted in lead sheathing and compressed under a triaxial load of 250 psi to seat the samples firmly in the sheath. Deformation of the samples was not observed during the loading. The samples were placed in a test cell and air was passed through the sample at a differential pressure, across the sample, of 15 psi. The air flow was measured and permeability was calculated from Darcy's Law. Since some samples were suspected of air leakage around the sheath, all samples were stripped of their sheaths and were mounted in plastic and rerun through the airflow measurements. About half of the samples showed a decrease in the permeability of 10%-50% but the other half showed little or no change. The values in Table I are the final results from the plastic mounting rerun.

Porosity:

The sediment samples were mounted in a sealed chamber and a volume of helium, equal to the volume of the sample chamber at 100 psi was introduced. The resulting chamber pressure was converted to grain volume of the sample using Boyle's Law. Bulk volume was measured by immersion of the sample in mercury. The porosity was calculated by dividing grain volume by bulk volume and subtracting this number from 100%.